

Physical Pedotransfer Functions To Compute Saturated Hydraulic Conductivity From Bimodal Characteristic Curves For A Range Of New Zealand Soils

Revision of Manuscript HESS-2016-636

RESPONSE TO EDITOR

Dear Prof. Nunzio Romano,

We would like to express, our gratitude for your efforts for organizing the review of our article: *Physical Pedotransfer Functions To Compute Saturated Hydraulic Conductivity From Bimodal Characteristic Curves For A Range Of New Zealand Soils*. We really appreciate your positive evaluation, and the feedback that you find our research interesting and valuable. We also wish to acknowledge the time and quality of Reviewer 1 and 3. In the revised version of the paper we employed the following major modifications:

- 1) We changed the title of the manuscript from "*Physical pedotransfer functions to compute saturated hydraulic conductivity from bimodal characteristic curves for a range of New Zealand soils*" to "*Saturated hydraulic conductivity model computed from bimodal water retention curves for a range of New Zealand soils*" to reflect that the developed K_s model is not a pedotransfer function but a K_s model. We also made some few changes in the introduction to reflect the change of the title.
- 2) We rewrote section 4.1. *Measurement of physical soil properties* where we provided more emphasis on the measurement method and removed details of methods used to sample the data which did not add value to the paper.
- 3) Provided better explanation of the relationship between H_{mac} and $h_{m,mac}$ (Eq. 15).
- 4) Improved the quality of the equations.

Yours sincerely,

Joseph Alexander Paul Pollacco, Trevor Webb, Stephen McNeill, Wei Hu, Sam Carrick, Allan Hewitt, Linda Lilburne

Physical Pedotransfer Functions To Compute Saturated Hydraulic Conductivity From Bimodal Characteristic Curves For A Range Of New Zealand Soils

Revision of Manuscript HESS-2016-636

RESPONSE TO REFEREE 1

Dear Reviewer 1,

We would like to express, our gratitude for your efforts for your review of our article: *Saturated hydraulic conductivity model computed from bimodal water retention characteristic curves for a range of New Zealand soils*. We really appreciate your positive evaluation. We also wish to acknowledge for the time and the efforts of your comprehensive review that helped us to significantly improve the manuscript.

MAJOR COMMENTS

However, the manuscript is fragmented in too many small parts and requires some minor improvement in its structure.

Thanks for bringing up this issue, to clarify the manuscript we simplified the subsections of the *Methods* section.

1) Subjective choice of $h_{m_mac}=3.16$ cm (Eq. 15) in absence of measurements of data points near saturation. Maybe in this case, it would be recommended to optimize h_{m_mac} in order to increase objectivity and add flexibility.

We agree that Eq. 15 needs further explanation and therefore we rewrote the section as follow:

$$h_{m_mac} = \exp \left[\frac{\ln(H_{mac})}{P_{m_mac}} \right] \quad (15)$$

where P_{m_mac} is a fitting parameter greater than 1. We found the fitted value of P_{m_mac} was 2.0, however this fitted parameter was very broadly determined. The cause might be that we are optimizing σ_{mac} and therefore h_{m_mac} and σ_{mac} might be linked. Linked parameters (Pollacco et al., 2008a, 2008b, 2009) means that there is an infinite combination of sets of linked parameters h_{m_mac} and σ_{mac} which produces values of objective function close to that obtained with the optimal parameter set and for which there exists a continuous relationship between h_{m_mac} and σ_{mac} . Further research needs to determine if having more data in the macropore domain would reduce the cause of non-uniqueness. To illustrate h_{m_mac} , the equivalent r_{m_mac} point is shown in Fig. 1, where r_{m_mac} is the inflection point of the macropore domain. Fig. 1 also shows that the matrix and the macropore domains meet at R_{mac} (H_{mac}).

2) The parameter W (“empirical” according to the authors) in the bimodal form of Romano et al. (2011) guarantees that the sum of the matrix and macropore domains gives $Se=1$ (same role as in Durner, 1994). The authors replace it with a new parameter (θ_{s_mac}). Indeed they state that this new parameter is “physically sound” and can be easily optimized with the other soil moisture parameters in the matrix range delimited by H_{mac} , that is empirically fixed at 10 cm. Isn’t it a contradiction? The authors should test this hypothesis on soil samples comprising measurements near saturation. This requires at least a few examples on soils taken from UNSODA or HYPRES for instance.

Thanks for your comments; nevertheless we do not fully understand why you believe there are contradictions. I improved the section and please inform us if it answers your concerns.

*The shape of $\theta_{bim}(h)$ is identical to that of $\theta_{bim_rom}(h)$, but the advantage of $\theta_{bim}(h)$ is that it uses the physical parameter θ_{s_mac} instead of the empirical parameter W , and $\theta_{s_mac} (\leq \theta_s)$ is **more easily** parameterized than W*

particularly when there is no available data in the macropore domain. When we do not have data in the macropore domain, θ_{s_mac} is determined by fitting the hydraulic parameters θ_{s_mac} , θ_r , h_m , σ of $\theta_{bim_mat}(h)$ (Eq. (10b)) solely in the matrix range ($r < R_{mac}$ or $h > H_{mac}$) Fig. 1 shows that R_{mac} and θ_{s_mac} delimit the matrix and the macropore domains and that r_m of the Kosugi model is the inflection point of $\theta_{bim_mat}(h)$ and r_{m_mac} is the inflection point of $\theta_{bim_mac}(h)$.

3) The RMSE-values obtained by this technique should be compared to the RMSE-values of existing methods (published in other articles) that estimate Ks from unimodal soil moisture parameters.

We agree that it will be best to compare our results with published data. We therefore compared our results to those of Pollacco et al., (2013):

The RMSE_{log10} of K_{s_uni} for subsoil is 0.47 cm day⁻¹ (Table 6) which is slightly worse compared to the RMSE_{log10} of 0.420 cm day⁻¹ by using UNSODA and HYPRES data sets (Pollacco et al., 2013).

4) Experimental design needs to be clear: The authors mention that the water content values were measured at the following matric potential points: 5, 10, 20, 40, 50, 100, 1500 kPa (Lines 296-297) please refer to the Book Methods of Soil Analysis, Part 4, Physical Methods” (J.H. Dane and G.C. Topp, eds.), pp. 692-698, SSSA Book Series N.5, Madison, WI, USA: which method was used to measure the moisture release curve? Hanging water column, suction tables, Pressure plate etc.

We agree that clarification of the experimental design is required and therefore we rewrote the section 4.1. *Measurement of physical soil properties*

MINOR COMMENTS:

1) I doubt the term “pedotransfer function” is proper to identify the estimate of Ks from water retention parameters

We agree that the meaning of pedotransfer function is not well defined so therefore we are happy to change the title to:

Saturated hydraulic conductivity model computed from bimodal water retention characteristic curves for a range of New Zealand soils

We also made some minor corrections in the introduction to clarify that we are dealing with a model and not with a pedotransfer function.

2) Line 21 page 1: specify if you refer 100 mm to diameter or something else

Yes, we agree we need further specification.

*The K_s data were collected using a small core size of 10 cm **diameter**.*

3) Line 27 page 1: I agree that there are uncertainties related to the core sizes, but eventual improvements should be tested on larger cores.

The manuscript purpose was to make the best out of the historical data stored in S-map <https://smap.landcareresearch.co.nz/> which contains large uncertainties. Nevertheless, based on the recommendations made in section 6. *Recommended future work to improve the New Zealand soil database* we are now in the phase of collecting new data sets by using large core of size and by taking more measurement close to saturation and we plan to publish the results in due course.

4) Line 63 page 2: add references

We added the following historical reference since to our understanding there does not seem to be a specific paper written by Poiseuille which relates to the Hagen-Poiseuille and Darcy law.

Anon: The History of Poiseuille’s Law, Annual Review of Fluid Mechanics, 25(1), 1–20, doi:10.1146/annurev.fl.25.010193.000245, 1993.

5) Line 144 and 168, page 5: why is it [0,1]?

This is a mathematical notation such that the feasible range is the internal interval including zero but not including one. This is because when $\tau_3=1$ then the K_s model returns NaN.

6) Lines 194-195, page 6: In Eqs 11b and 11c the two integral ranges are both $S_e=[0,1]$. Shouldn't they be $S_e=[0, S_{e_mac}]$ and $[S_{e_mac}, 1]$?

The reviewer's question is to determine if in the matrix domain the integral should go from $[0, S_{e_mac}]$ and in the macropore domain the integral should go to $[S_{e_mac}, 1]$ compared to the two integrals evaluated over the interval $S_e=[0,1]$. This was questioned during the development of the model, and we decided to use the simplified notation for which the two integrals go to $S_e=[0,1]$ because numerically it makes little difference since the pore size distribution of the macropore and the matrix do not overlap since we constrained by $\sigma_{mac} < 1.5$.

7) Lines 250-254, page 8: The determination of saturated water content (namely θ_s) is rather easy, why do the authors use the artefact of Eq.6?

In the section 4.1 *Measurement of physical soil properties* we explained that the historical data used in this study had some issues in measuring θ_s , this is why we used Eq. 6:

“The total porosity, ϕ , described in Eq. (5) contains uncertainties from the measurement methods, where ϕ is derived from separate measurements of particle density and bulk density, rather than being directly measured”.

8) Fig. 2 page 25: improve overall quality, enlarge fonts

We improved the quality of Figure 2.

9) Fig. 3 page 26: please add the 1:1 line. Fig. 3 and 4 should be the same size

We added the 1:1 line in the caption. It is not possible that Fig.3 and Fig.4 are the same size since they were designed by using different software: Fig. 3 was designed by using PyX (Python) and Fig 4 by using R.

10) I encourage the authors to investigate on possible relationships between tortuosity parameters and soil physical parameters (texture, porosity etc)

We are currently collecting a new set of data where we are specifically measuring near saturation collected by using large cores, and we will investigate relationship between tortuosity parameters and other soil physical parameters.

Physical Pedotransfer Functions To Compute Saturated Hydraulic Conductivity From Bimodal Characteristic Curves For A Range Of New Zealand Soils

Revision of Manuscript HESS-2016-636

RESPONSE TO REFEREE 2

Dear Reviewer 2,

We would like to express, our gratitude for your efforts for your review of our article: *Saturated hydraulic conductivity model computed from bimodal water retention characteristic curves for a range of New Zealand soils*. We understand that you have concerns about the manuscript and we hope that we have addressed them.

The intent of this paper is not very clear. On closer examination, even the title of the paper is problematic to me.

We modified the title of the paper as suggested by reviewers 1 & 3 since they argue that the developed K_s model is not a pedotransfer function but a functional model so therefore we changed the title to:

Saturated hydraulic conductivity model computed from bimodal water retention characteristic curves for a range of New Zealand soils

1. It is true that soil moisture release curve, $\theta(h)$, is still being measured in the laboratory despite being time-consuming. The hydraulic conductivity function $K(h)$ is too expensive and time-consuming to measure and is typically reconstructed from the saturated hydraulic conductivity K_s and $\theta(h)$. Therefore what the authors seem to suggest in the paper is to use a bimodal $\theta(h)$ to compute K_s . The error involved will be too huge. In fact, it is common knowledge that an accurate $K(h)$ can be obtained by measuring K_s and $\theta(h)$ rather than by estimating $K(h)$ directly from $\theta(h)$. In fact, this is one C1 of the recommendations for future work in the paper. 2. Saturated K_s is not more time-consuming to measure compared to $\theta(h)$.

The reviewer raises an important issue. In some cases, $\theta(h)$ can be easier to measure, but our collective field and laboratory experience over many years is that the components of measurement required to estimate K_s are more expensive to measure accurately, given the great variability we commonly expect for this property in New Zealand soils. We believe that this is due to the relatively young geomorphic development of the soils in this country. The purpose of this paper is to test one approach for modelling the $K(h)$ curve, which is an established valid approach in the scientific literature. You are correct that there are alternative approaches, which we will test in time as part of the S-map programme in NZ, but it is not the purpose of this paper to test these other options.

For clarification, among our *recommendations for future work* is a task to collect more accurate information on $\theta(h)$ and $K(\theta)$ to improve the development of K_s models, which are required for the predictions of $K(\theta)$ to be fed into the S-map data base (<https://smap.landcareresearch.co.nz/>).

3. The approach chosen to determine K_s is strange as K_s depends on the voids in the soil. I can understand if one chooses the particle size distribution as providing the key parameters in a pedotransfer function to estimate K_s . Using $\theta(h)$ is an indirect process of getting the pore-size distribution but due to the time-consuming nature of the test, it is less suitable to be used as a proxy for pore-size distribution.

As mentioned above, the purpose of this paper is to test one approach for modelling the $K(h)$ curve, which is an established valid approach in the scientific literature. You are correct that there are alternative approaches, which we will test in time as part of the S-map programme in NZ, but it is not the purpose of this paper to test these other options.

Thanks for providing us with new insight in the development of K_s model based on the particle size distribution. Nevertheless, the current S-map database does not have accurate particle size distribution, nevertheless we have good data on $\theta(h)$ and this is why we decided to use $\theta(h)$ to infer the pore size distribution based on Eq. 1. It will be interesting to compare K_s models based on $\theta(h)$ and models based on particle size distribution for which, to my best of knowledge, a comparison has not yet been published.

For instance, Arya and Paris (1981) showed that there is a strong relationship between pore-size distribution and the particle-size distribution and therefore adding soil texture information should not improve the model.

4. Even when using $\theta(h)$, it is expected that the matrix (micro) pores are the ones governing K_s but this is not evident from the paper.

The percentage of pores contributing to macropores as discussed in the paper depends largely on $\theta_s - \theta_{s_mac}$.

5. The error for K_s shown in Figures 3 and 4, is about +/- one order. The errors in the measurement of K_s should be less despite the problems mentioned in Section 4.1.3.

This may suggest that the model is performing more accurately than the measured data! As mentioned in the paper high variability in K_s is widely recognised in the literature, which is why we are suggesting in the paper that future work use larger sample volumes (which is also shown in the literature to reduce measurement variability).

6. Based on the above assessment, most of the equations presented in the paper have little value. In addition, none of the equations presented is a pedotransfer function in the traditional sense.

As mentioned above, the purpose of this paper is to test one approach for modelling the $K(h)$ curve, which is an established valid approach in the scientific literature. As discussed, we changed the title of the paper to reflect our agreement that our K_s model does not fit in the category of pedotransfer function but in the category of a model which is derived from principles of soil physics.

It is important to remember that the ultimate purpose of this paper is to derive K_s from $\theta(h)$ data which is available in S-map, which is the national soil database of New Zealand. S-map addresses key issues that are important to New Zealand soils, although the methodology could in principle be applied elsewhere, and therefore the developed equations are useful to a greater or lesser extent outside New Zealand, depending on the soil information available other countries.

7. More relevant literature on estimating of saturated hydraulic conductivities should be cited e.g.

Many thanks for proposing literature to enrich our paper we included them in our paper. We found the following references to be highly relevant to this topic:

Chapuis, R.P. (2004) Predicting the saturated hydraulic conductivity of sand and gravel using effective diameter and void ratio. Canadian Geotechnical Journal, 2004, 41:787-795, 10.1139/t04-022

Mbonimpa, M., Aubertin, M., Chapuis, R.P. (2002) Practical pedotransfer functions for estimating the saturated hydraulic conductivity. Geotechnical and Geological Engineering (2002) 20: 235. doi:10.1023/A:1016046214724

Physical Pedotransfer Functions To Compute Saturated Hydraulic Conductivity From Bimodal Characteristic Curves For A Range Of New Zealand Soils

Revision of Manuscript HESS-2016-636

RESPONSE TO REFEREE 3

Dear Reviewer 3,

We would like to express, our gratitude for your efforts for your review of our article: *Saturated hydraulic conductivity model computed from bimodal water retention characteristic curves for a range of New Zealand soils*. We really appreciate your positive evaluation. We also wish to acknowledge for the time and the efforts of your comprehensive review that helped us to significantly improve the manuscript.

I would recommend considering modifying the title, because the presented method is closer to a model describing the Ks than to a PTF.

We agree that the meaning of pedotransfer function is not well defined so therefore we are happy to change the title to:

Saturated hydraulic conductivity model computed from bimodal water retention characteristic curves for a range of New Zealand soils

We also made some minor corrections in the introduction to clarify that we are dealing with a functional model and not a pedotransfer function.

TEXT

Line 11: here and in the entire text instead of “moisture release” “moisture retention” is more frequently used in the literature, therefore it might be more preferable to use.

We agree and are happy to systematically replace *moisture retention* in the manuscript with *moisture release*.

Line 18: here and in the entire text please use “structured soil” instead of “structural soil” if soil having aggregates is referred.

We agree and are happy to systematically replace “*structured soil*” instead of “*structural soil*” in the manuscript where appropriate.

Line 42: please refer to more recent PTFs.

We added a recent PTF reference developed in New Zealand:

Cichota, R., Vogeler, I., Snow, V. O., and Webb, T. H.: Ensemble pedotransfer functions to derive hydraulic properties for New Zealand soils, Soil Research, 51, 94–111, doi:10.1071/sr12338, 2013.

Line 94-95: it would be helpful for the reader to highlight what r and r_m means. If r_m refers to the mean of soil-pore radius I would suggest writing r with overbar. If σ means the variance of the log transformed soil-pore radius, please make it clear in the notation.

To clarify the meaning of the Kosugi parameters we rephrased Eq. 1 as follow:

where θ_r and θ_s [$\text{cm}^3 \text{cm}^{-3}$] are the residual and saturated water contents, r_m [cm] is the median pore radius and σ [-] denotes the standard deviation of $\ln(r)$.

Line 104: it might worth to give a number for the equation $r=Y/h$, than it is easier to refer it in 8b.

As in the recent paper *Using Bimodal Lognormal Functions to Describe Soil Hydraulic Properties* published by Romano et al., (2011) they did not include an equation number for the Young–Laplace capillary equation since it is understood that all soil scientist reading this specialized paper would be familiarised with the Young–Laplace capillary equation. Nevertheless, for clarity I added the following note in Eq. 8b:

I added

$$r_m = Y/h_m \text{ (Young–Laplace capillary equation)}$$

Line 107: it might increase the readability/understanding if another notation would be used for the mean and standard deviation of $\ln(h_{m_mac})$. If first \ln of h_{m_mac} is calculated and then the mean and standard deviation of the transformed h_{m_mac} , than the present notation does not tell it. Please check it.

To clarify the meaning of the Kosugi parameters we rephrased Eq. 3 as follow:

where h_m [cm] is the median metric head

Lines 134-146: I hope that I didn't miss anything in Eq. 7-8b, if yes, sorry, just would like to clarify it. It seems that you have a small mistyping in the numbering of the equations, in line 146 you refer to Eq. 8 which is Eq. 7 in the text, Eq. 8 is missing. Please correct it in the entire manuscript.

Thanks for noting this issue in the manuscript. We did not find any further issues of the numbering.

If S_e equals to 1 in Eq. 7 as mentioned in line 146, why is it included after K_s which in theory tells already that it is a saturated state because you use the notation "s"? If it is needed to follow the mathematical logic, a possible solution might be to add $S_e=1$ under Eq. 7. If it is stated could Eq. 8a, 8b, 11a-14b, 19 be simplified?

Just to clarify we defined in 2.1 *Kosugi unimodal characteristic water retention and unsaturated hydraulic conductivity curve* $S_e(r) = (\theta - \theta_r)/(\theta_r - \theta_s)$.

We took on board your simplifications by rewriting Eq. 8, 11, 14 and 19 by integrating between 0 and 1 instead of 0 and S_e . I also simplified the notation for e.g. by replacing $K_{s_bim}(S_e)$ to K_{s_bim} . Nevertheless, we do not see how mathematically we can further simplify the equations.

Lines 154 and 174: I would suggest to use "bimodal water retention curve" instead of "bimodal characteristic curve" to make it completely clear for the readers that you have to deal with both water retention curve ($\Theta(h)$) and hydraulic conductivity curve ($K(\Theta)$).

Thanks for improving the manuscript, we agree that replacing "bimodal characteristic curve" throughout the manuscript with "bimodal water retention curve" clarifies the meaning.

Line 162: please give the terminology of H_{mac} too – as you did it for R_{mac} .

Thanks for helping us to clarify the manuscript, we made the modifications as suggested.

R_{mac} is the theoretical pore size r that delimits macropore and matrix flow and H_{mac} is the theoretical pressure that delimits macropore and matrix flow

Line 167: same as in line 107. Please check it.

As suggested we made the following modifications.

where θ_s , h_{m_mac} and σ_{mac} are, respectively, the saturated water content, the median pore radius and the standard deviation of $\ln(h)$ of the macropore domain, θ_r , h_m and σ are parameters of the matrix domain, and W is a constant in the range $[0,1)$.

Line 226: maybe I miss something, for me it is not clear why 2 and why not 1.5. Can you please describe it?

We agree that Eq. 15 needs further explanation and therefore we rewrote the section as follow:

$$h_{m_mac} = \exp \left[\frac{\ln(H_{mac})}{P_{m_mac}} \right] \quad (15)$$

where P_{m_mac} is a fitting parameter greater than 1. We found the fitted value of P_{m_mac} was 2.0, however this fitted parameter was very broadly determined. The cause might be that we are optimizing σ_{mac} and therefore h_{m_mac} and σ_{mac} might be linked. Linked parameters (Pollacco et al., 2008a, 2008b, 2009) means that there is an infinite combination of sets of linked parameters h_{m_mac} and σ_{mac} which produces values of objective function close to that obtained with the optimal parameter set and for which there exists a continuous relationship between h_{m_mac} and σ_{mac} . Further research needs to determine if having more data in the macropore domain would reduce the cause of non-uniqueness. To illustrate h_{m_mac} , the equivalent r_{m_mac} point is shown in Fig. 1, where r_{m_mac} is the inflection point of the macropore domain. Fig. 1 also shows that the matrix and the macropore domains meet at $R_{mac}(H_{mac})$.

Line 235: Please describe shortly or rephrase what do you mean by main horizon?

We removed the following sampling description since it is confusing and it does not add extra clarifications to the results:

~~Three horizons in each soil profile were sampled from deep soils (topsoil, horizon with slowest permeability, and the main horizon between these) and two from shallow soils (topsoil and the main horizon above gravels).~~

Lines 236, 237: in case of undisturbed samples please provide the volume of the core.

We rewrote the 4.1. Measurement of physical soil properties section and we provided extra details of the field and laboratory methods

Lines 247,248: please use cm also here.

For consistency, we changed mm to cm in all the manuscript.

Line 251: please refer which method was used to measure particle density.

This was already mentioned in the manuscript:

Laboratory analysis for particle size followed Gradwell (1972).

Line 259: please use cm also here.

You are right for consistency with the rest of the text we changed mm to cm in all the manuscript.

Line 262: point a) does not fit into the uncertainty due to measurement error. It increases the error of the model, therefore better to mention it later when the performance of the bimodal model is analysed.

The variability in both θ and K_s reflect variation within the stratum of a supposedly-uniform soil type. The effect is magnified by the small cores used, so in this sense it is an artefact of the measurement process and it is measurement error in the classical sense. We introduced this point in order to inform the reader concerning these historical datasets, which are considerably less accurate than modern datasets and that the reader should understand that if we had modern datasets the K_s model should be much better.

Line 279-280: “anthropogenic disturbance and biological activity” might cover better the disturbances influencing soil porosity.

This is much better and concise; we implemented the corrections in to the manuscript.

Line 287: Eq. 10c is called “modified Romano bimodal” curve, why is it called unimodal Kosugi here?

We believe that we did not make any typos since Eq. 10 does not use the empirical weighting so it is no longer $\theta_{bim_rom}(h)$.

Line 290: please describe shortly how you optimized K_{s_uni} and K_{s_bim} models. Which measured parameters did you use?

If I understand properly your comments, you wanted us to provided further explanation on the objective function which is described below.

Optimization of the τ_1 , τ_2 , τ_3 of the K_{s_uni} model (Eq. (8)) and τ_{1_mac} , τ_{2_mac} , τ_{3_mac} , σ_{mac} parameters of the K_{s_bim} models (Eq. (14)), where the physical feasible ranges of the tortuosity parameters are described in Table 3.

Line 302: could you provide reference or short explanation on why power was set to 6?

The computation of K_{s_bim} requires $\theta(h)$ to be accurate near saturation, when the drainage is mostly from large pores, and to achieve **this balance we found by trial and error that best results are achieved** when $P_{ower} = 6$.

Lines 307: instead of $K(\theta)$ is not it more correct to write K_s ? If yes, please rephrase sentence in lines 308-309.

The log transformation of OF_{ks} puts more emphasis on the lower K_s and therefore reduces the bias towards larger conductivity

Lines 319-322: it might worth to rephrase this section or include them separately under the subsections.

For clarity we provide at the beginning of the *Result and discussion* section the plan of the layout of the results.

Line 321: please include if the difference is significant between unimodal and bimodal K_s models.

We commented below in section 5.2 *Improvement made by using K_{s_bim} instead of K_{s_uni}*

Line 322-324: please include it in “materials and methods” section

Thanks for your recommendation we moved the equation of goodness of fit into the *material and methods*.

Lines 326-330 and 332-335 are not totally in line, please harmonize them.

If you are talking about the tabs than I lined them up. Thanks.

Lines 341-344: is the improvement significant – overall or only in case of subsoils? Please include it in the text.

The improvement is more significant in the topsoil than for the subsoil. We made a minor modification to the text to improve clarification:

*As expected, the **reasonable** improvement is greater for topsoil containing higher macroporosity (12% improvement) than for subsoil (4% improvement)*

Line 410: there is a mistyping, please delete “improved” before “Romano $\theta(h)$ ”. Please include the results of the modified bimodal model (10a) compared to Romano’s model under “results” section too.

We agree that the wording was incorrect, we did not improve the model we just changed the form of parameterizing the model. Since the shape of the two models are identical we do not need to compare Romano $\theta(h)$ with $\theta(h)$ bimodal.

*We report here on further adaptations to the saturated hydraulic conductivity model to suit it to dual-porosity structured soils (Eq. 10) by computing the soil water flux through a continuous function of a **modified version** of Romano et al. (2011) $\theta(h)$ dual pore-size distribution (Eq. 18). The shape of the Romano $\theta(h)$ distribution is identical to the **modified** $\theta(h)$, but the advantage of the developed bimodal $\theta(h)$ is that it is more easily parameterized when no data are available in the macropore domain.*

Line 424: please include for what kind of soils you suggest to use the presented model and what are the limitations of its use.

This is indeed a valid question, but to answer this question correctly we would need to collect more soils samples in each subgroup (Table 4). Based on the section “*Recommended future work to improve New Zealand soil database*” we believe that the greatest challenge is to make predictions on slowly permeable soils as mentioned:

Therefore, this model's performance may be restricted in cases of non-Darcy flow, such as non-laminar and turbulent flow, which may occur in large macropores.

Make more accurate measurements on slowly permeable soils ($< 1 \text{ cm day}^{-1}$), which are important for management purposes but are not well represented in the current databases.

TABLES

Line 540: please rephrase, possible solution: " θ_5 which is". Why is θ_5 the minimum value of θ_s ?

Due to uncertainties in measuring θ_s , we optimized θ_s . The feasible range of $0.6 > \theta > \theta_5$. Since as mentioned *The closest data point near saturation is $\theta(h = 50 \text{ cm})$, which is in the matrix pore space.*

Lines 545-546: "When τ_3 increases the connectivity of the soil increases", it seems to be in contradiction with lines 150-151 a 5th row of Table 3.

We total agree with you this is why in section *Optimal tortuosity parameters* I commented on this contradiction:

The optimal tortuosity parameters of K_{s_bim} and K_{s_uni} (Table 6) show that the optimal parameters are within the physically feasible limits, except for τ_{3_mac} of the subsoil, which are greater than τ_3 . This is understandable because Pollacco et al. (2013) found τ_3 not to be a very sensitive parameter.

Lines 555-558: please rephrase title of the table and its content because it is not clear in present from without reading the main text of the manuscript.

We improved table 5 and the caption description.

FIGURES

Figure 3 and 4 has similar content, please consider including them under 1 figure caption maybe including a) and b) figures.

Thanks for suggesting merging figure 3 and figure 4. Since figure 3 relates to section *Improvement made by using K_{s_bim} instead of K_{s_uni}* and figure 4 relates to section *Uncertainty of the bimodal saturated hydraulic conductivity model predictions*, merging the 2 figures would give the wrong interpretation to the reader.

Technical corrections

Just a small suggestion, in Eq. 11a-11c and 12-13 maybe you can start with models regarding the macropore and then follow with the matrix similarly to Eq. 10a-10c, 14a-14b and 19, in this way you would have the same order in the equations in the entire manuscript.

Thanks for spotting this inconsistency, I will change the order of the equations mentioned starting from matrix than following for macropore. It is easier to start the explanations for matrix than for macropore.

Please check Eq. 11a, 11b and 11c, because they have different size that other equations.

Yes we corrected the quality of the equations and they now have the same size.

Line 322: please put log10 in subscript.

Thanks for spotting this typo:

1

2 ~~Physical pedotransfer functions to compute s~~**Saturated hydraulic**
3 **conductivity model computed from bimodal water retention**
4 **~~characteristic~~ curves for a range of New Zealand soils**

5 Joseph Alexander Paul Pollacco¹, Trevor Webb¹, Stephen McNeill¹, Wei Hu², Sam Carrick¹, Allan
6 Hewitt¹, Linda Lilburne¹

7 ¹ Landcare Research, PO Box 69040, Lincoln 7640, New Zealand

8 ² New Zealand Institute for Plant & Food Research Limited, Private Bag 4704, Christchurch 8140, New Zealand

9 Correspondence to: Joseph A.P. Pollacco (Pollacco.water@gmail.com)

10

11 **Abstract.** Descriptions of soil hydraulic properties, such as *soil moisture retention curve*, $\theta(h)$, and *saturated hydraulic*
12 *conductivities*, K_s , are a prerequisite for hydrological models. Since the measurement of K_s is expensive, it is frequently
13 derived from pedotransfer functions. Because it is usually more difficult to describe K_s than $\theta(h)$ from pedotransfer
14 functions, Pollacco et al. (2013) developed a physical unimodal model to compute K_s solely from hydraulic parameters
15 derived from the Kosugi $\theta(h)$. This unimodal K_s model, which is based on a unimodal Kosugi soil pore-size distribution, was
16 developed by combining the approach of Hagen-Poiseuille with Darcy's law and by introducing three tortuosity parameters.
17 We report here on (1) the suitability of the Pollacco unimodal K_s model to predict K_s for a range of New Zealand soils, and
18 (2) further adaptations to this model to adapt it to dual-porosity structured soils for soils having aggregates by computing the
19 soil water flux through a continuous function of an improved bimodal pore-size distribution. The improved bimodal K_s
20 model was tested with a New Zealand data set derived from historical measurements of K_s and $\theta(h)$ for a range of soils
21 derived from sandstone and siltstone. The K_s data were collected using a small core size of 10 cm diameter, causing large
22 uncertainty in replicate measurements. Predictions of K_s were further improved by distinguishing topsoils from subsoil.
23 Nevertheless, as expected stratifying the data with soil texture only slightly improved the predictions of the physical K_s
24 models because the K_s model is based on pore-size distribution and the calibrated parameters were obtained within the
25 physically feasible range. The improvements made to the unimodal K_s model by using the new bimodal K_s model are modest
26 when compared to the unimodal model, which is explained by the poor accuracy of measured total porosity. Nevertheless,
27 the new bimodal model provides an acceptable fit to the observed data. The study highlights the importance of improving K_s
28 measurements with larger cores.

29

30

31 **Keywords.** saturated hydraulic conductivity; bimodal; Kosugi model; soil moisture retention curves; pedotransfer functions;
32 tortuosity; Hagen-Poiseuille; soils; New Zealand; S-map

33

34 **Abbreviations.** PTFs: statistical pedotransfer functions; S-map: New Zealand soil database; $\theta(h)$ soil moisture retention
35 curve; K_s saturated hydraulic conductivity

36

37 1 Introduction

38 Modelling of the water budget, irrigation, and nutrient and contaminant transport through the unsaturated zone requires
39 accurate soil moisture retention, $\theta(h)$, and unsaturated hydraulic conductivity, $K(\theta)$, curves. The considerable time and cost
40 involved in measuring $\theta(h)$ and $K(\theta)$ directly for a range of soils mean that the information for specific soils of interest is
41 often not available (Webb, 2003). Therefore, these curves are generally retrieved from pedotransfer functions (PTFs), which
42 are statistical relationships that generate lower-precision estimates of physical properties of interest based on many rapid and
43 inexpensive measurements (e.g., Balland and Pollacco, 2008; Pollacco, 2008; Anderson and Bouma, 1973; Webb, 2003,
44 Cichota et al., 2013).

45
46 The S-map database (Lilburne et al., 2012; Landcare Research, 2015) provides soil maps for the most intensively used
47 land in New Zealand and is being gradually extended to give national coverage. S-map provides data for extensively used
48 soil models, such as the soil nutrient model OVERSEER and the daily simulation model APSIM used by agricultural
49 scientists. McNeill et al. (2012) used the New Zealand National Soils Database to derive PTFs to estimate $\theta(h)$ at five
50 tensions from morphological data of soils mapped in S-map. One of the current weaknesses of S-map is a lack of capacity to
51 estimate $K(\theta)$. Building on the work of Griffiths et al. (1999), Webb (2003) showed that morphologic descriptors for New
52 Zealand soils can be used to predict K_s . However, the predictions of K_s were found to be too coarse for application to the
53 wide range of soils within S-map. Therefore, Cichota et al. (2013) tested published statistical PTFs developed in Europe and
54 the USA to predict $\theta(h)$ and $K(\theta)$ for a range of New Zealand soils. They combined the best two or three PTFs to construct
55 ensemble PTFs. They considered the ensemble PTF for $\theta(h)$ to be a reasonable fit, but the ensemble PTF for estimating K_s
56 exhibited large scatter and was not as reliable. The poor performance when estimating K_s was possibly due to the absence of
57 any measurements of pore-size distribution in their physical predictors (Watt and Griffiths, 1988; McKenzie and Jacquier,
58 1997; Chapuis, 2004; Mbonimpa et al., 2002), and also to the large uncertainties in the measurements from small cores
59 (McKenzie and Cresswell, 2002; Anderson and Bouma, 1973). Consequently, there is an urgent need in New Zealand to
60 develop a physically based ~~pedotransfer function (PTF) model for K_s model which that~~ is based on pore-size distribution.

61
62 Since PTFs developed to characterize $\theta(h)$ are more reliable than PTFs to characterize $K(\theta)$ (e.g., Balland and Pollacco,
63 2008; Cichota et al., 2013), Pollacco et al. (2013) developed a new ~~class of~~ physical ~~pedotransfer function, PTF, model~~ that
64 predicts unimodal K_s solely from hydraulic parameters derived from the Kosugi (1996) $\theta(h)$. The ~~K_s PTFs model are is~~
65 derived by combining the Hagen-Poiseuille and Darcy law (Anon., 1993) and by incorporating three semi-empirical
66 tortuosity parameters. The model is based on the soil pore-size distribution and has been successfully validated using the
67 European HYPRES (Wösten et al., 1998; Wösten et al., 1999; Lilly et al., 2008) and the UNSODA databases (Leij et al.,
68 1999; Schaap and van Genuchten, 2006), but has not yet been applied to New Zealand soils. Most New Zealand soils are
69 considered to be structured, with two-stage drainage (Carrick et al., 2010; McLeod et al., 2008) and bimodal pore-size
70 distribution (e.g. Durner, 1994). Romano and Nasta (2016) showed by using the HYDRUS-1D package that large errors
71 arise in the computation of the water fluxes if unimodal $\theta(h)$ and $K(\theta)$ are used in structured soils. We therefore propose to
72 improve the unimodal Pollacco et al. (2013) ~~K_s PTF~~-model so that it can predict K_s for structured soils with bimodal
73 porosity.

74
75 Measured K_s values are widely recognised as one of the most variable soil attributes (McKenzie and Cresswell 2002;
76 Carrick, 2009). exhibit high variability (Webb et al., 2000, Carrick, 2009). This is also recognised for New Zealand soils,
77 both due to the high variability over short distances in soil parent material, age, depth and texture, was well as strong

macropore development with preferential macropore flow recognised as the norm rather than the exception in New Zealand soils (Webb et al., 2000; Carrick, 2009; McLeod et al., 2008) especially true on the Canterbury Plains of the eastern South Island of New Zealand where the extensive lowland consist of a series of coalescing fans built up by abandoned braided river floodplains (Forsyth et al 2008, Cox and Barrell 2007). They include moderately to poorly sorted, boulder, sandy and silty rounded glacial outwash gravels close to moraine, and moderately to well sorted sandy, rounded gravel within the alluvial valley and plain deposits. Measured K_s values exhibit notoriously high variability (Carrick, 2009). The measurement variability is also expected to increase as the sampling diameter decreases because small cores provide an unrealistic representation of the abundance and connectivity of macropores (McKenzie and Cresswell, 2002; Anderson and Bouma, 1973). McKenzie and Cresswell (2002) suggest that the standard Australian laboratory measurements should use cores with minimum diameter of 25 cm and 20 cm length, of between 10–30 cm, with 25 cm. Australian research adapted the standard dimension of diameter of 20 cm and length of 2 diameter and 20 cm length the standard dimensions for Australian research. In New Zealand, K_s has been obtained by using small cores, commonly with 10 cm diameter and 7.5 cm length. This has contributed to very high variability in measured K_s (Webb et al., 2000).

The objectives of this research were to:

- test the suitability of the unimodal Pollacco et al. (2013) K_s model to predict K_s from New Zealand soils
- develop a K_s bimodal model that makes predictions in structured soils solely from hydraulic parameters derived from the Kosugi $\theta(h)$
- derive the uncertainties of the predictions of the K_s bimodal model
- provide recommendations on the critical data sets that are required to improve the S-map database in New Zealand.

2 Background

2.1 Kosugi unimodal water retention and unsaturated hydraulic conductivity curve

There are a number of closed-form unimodal expressions in the literature that compute the soil moisture retention curve $\theta(h)$ and the unsaturated hydraulic conductivity $K(\theta)$ curves, such as the commonly used van Genuchten (1980) and Brooks and Corey (1964) curves. We selected the physically based Kosugi (1996) closed-form unimodal log-normal function expression of $\theta(h)$ and $K(\theta)$ because its parameters are theoretically sound and relate to the soil pore-size distribution (Hayashi et al., 2009). Soils have a large variation in pore radius, r , which follows a log-normal probability density function. The unimodal Kosugi log-normal probability density function of pore radius (r) is often written in the following form:

$$\frac{d\theta}{dr} = \frac{\theta_s - \theta_r}{r\sigma\sqrt{2\pi}} \exp\left\{-\frac{[\ln(r/r_m)]^2}{2\sigma^2}\right\} \quad (1)$$

where θ_r and θ_s [$\text{cm}^3 \text{cm}^{-3}$] are the residual and saturated water contents, respectively; $\ln(r_m)$ [cm] is the median pore radius and σ [-] denotes the standard deviation of $-\ln(r)$ are the mean and variance of the log-transformed soil pore radius, $-\ln(r)$, respectively.

Let S_e denote the effective saturation, defining $S_e(r) = (\theta - \theta_r)/(\theta_r - \theta_s)$, such that $0 \leq S_e \leq 1$. Integrating Eq. (1) from 0 to r yields the unimodal water retention curve as a function of r :

$$S_e(r) = \frac{1}{2} \operatorname{erfc}\left[\frac{\ln r_m - \ln r}{\sigma\sqrt{2}}\right] \quad (2a)$$

113 with $r = \frac{r_m}{\exp\left[\operatorname{erfc}^{-1}\left[2 S_e\right] \sigma \sqrt{2}\right]}$ (2b)

114 where erfc is the complementary error function.

115

116 The Young–Laplace capillary equation relates the soil-pore radius, r , to the equivalent *matric suction head*, h (cm), at
 117 which the pore is filled or drained (i.e., $r = Y/h$, where $Y = 0.149 \text{ cm}^3$). Kosugi’s unimodal *moisture retention curve* $\theta_{\text{uni}}(h)$
 118 can be written in terms of S_e :

119 $S_e(h) = \frac{1}{2} \operatorname{erfc}\left[\frac{\ln h - \ln h_m}{\sigma \sqrt{2}}\right]$ (3)

120 where $\ln(h_m [\text{cm}])$ is the median metric head and σ represent the mean and standard deviation of $\ln(h)$, respectively.

121

122 The unimodal Kosugi unsaturated hydraulic conductivity function $K(\theta)$ is written as:

123 $K(S_e) = K_s \sqrt{S_e} \left\{ \frac{1}{2} \operatorname{erfc}\left[\operatorname{erfc}^{-1}(2S_e) + \frac{\sigma}{\sqrt{2}}\right] \right\}^2$ (4)

124 where K_s (cm day^{-1}) is the saturated hydraulic conductivity.

125

126 θ_s is computed from the total porosity, ϕ , which is deduced from *bulk density* (ρ_b) and *soil particle density* (ρ_p) as follows:

127 $\phi = \left[1 - \frac{\rho_b}{\rho_p} \right]$ (5)

128 Due to air entrapment, θ_s seldom reaches saturation of the total pore space ϕ (Carrick et al., 2011). Therefore, to take into
 129 account the fact that not all pores are connected, we perform the following correction of ϕ with α in the range [0.9, 1]:

130 $\theta_s = \alpha \phi$ (6)

131 It is accepted that $\alpha = 0.95$ (Rogowski, 1971; Pollacco et al., 2013; Haverkamp et al., 2005; Leij et al., 2005), but in this
 132 study the optimal α was found to be 0.98, since using a value of 0.95 resulted in several soil samples with θ_s (θ measured
 133 at 5 kPa) greater than θ_s , which is not physically plausible. This was due to the inaccuracy of measuring ϕ (discussed in
 134 Sect. 4.1.2).

135 The feasible range of the Kosugi hydraulic parameters is summarized in Table 1. The h_m and σ feasible range is taken
 136 from Pollacco et al. (2013), who combined data from the HYPRES (Wösten et al., 1998; Wösten et al., 1999; Lilly et al.,
 137 2008) and UNSODA (Leij et al., 1999; Schaap and van Genuchten, 2006) databases.

138

139 **Table 1. please insert here**

140 2.2 Pollacco unimodal saturated hydraulic conductivity model

141 The *saturated hydraulic conductivity* model, K_{s_uni} (Pollacco et al., 2013) computes K_s from the Kosugi parameters θ_s , θ , σ
 142 and h_m (or r_m). K_{s_uni} is based on the pore-size distribution (Eq. (1)) and the tortuosity of the pores. K_{s_uni} was derived by

143 adopting the method of Childs and Collisgeorge (1950) and modelling the soil water flux through a continuous function of
 144 Kosugi (1996) pore-size distribution. This was performed by combining the Hagen-Poiseuille equation (Anon, 1993) with
 145 Darcy's law and introducing the connectivity and tortuosity parameters τ_1 , τ_2 of Fatt and Dykstra (1951) and τ_3 of Vervoort
 146 and Cattle (2003). K_{s_umi} is computed as:

$$147 \quad K_{s_umi} = C (1 - \tau_1) (\theta_s - \theta_r)^{\frac{1}{1-\tau_3}} \int_0^1 r^{2(1-\tau_2)} dS_e \quad (7)$$

$$148 \quad \text{with } C = \frac{1}{8} \frac{\rho_w g}{\eta}$$

149 where for water at 20°C, density of water $\rho_w = 0.998 \text{ g cm}^{-3}$, acceleration due to gravity $g = 980.66 \text{ cm s}^{-2}$, dynamic viscosity
 150 of water $\eta = 0.0102 \text{ g cm}^{-1} \text{ s}^{-1}$ and C is a constant equal to $1.03663 \times 10^9 \text{ cm day}^{-1}$.

151
 152 Integrating with S_e instead of r avoids the complication of finding the minimum and maximum value of r . Isolating r of
 153 Eq. (2b) and replacing it in Eq. (7) gives:

$$154 \quad K_{s_umi}(S_e) = C (1 - \tau_1) (\theta_s - \theta_r)^{\frac{1}{1-\tau_3}} \int_0^1 \left\{ \frac{Y/h_m}{\exp \left[\operatorname{erfc}^{-1}(2 S_e) \sigma \sqrt{2} \right]} \right\}^{2(1-\tau_2)} dS_e \quad (8a)$$

$$155 \quad \text{or } K_{s_umi} = C (1 - \tau_1) (\theta_s - \theta_r)^{\frac{1}{1-\tau_3}} \int_0^1 \left\{ \frac{r_m}{\exp \left[\operatorname{erfc}^{-1}(2 S_e) \sigma \sqrt{2} \right]} \right\}^{2(1-\tau_2)} dS_e \quad (8b)$$

156 and $r_m = Y/h_m$ (Young-Laplace capillary equation)

157 where τ_1 , τ_2 , τ_3 are tortuosity parameters [0–1].

158 **Note that $K_s = K_{s_umi}(S_e = 1)$ (Eq. (8)).** If tortuosity were not included (τ_1 , τ_2 , $\tau_3 = 0$), the pore-size distribution model
 159 would mimic the permeability of a bundle of straight capillary tubes. Vervoort and Cattle (2003) state: “*In reality soils are*
 160 *much more complex, with twisted and crooked pores, dead-ending or connecting to other pores. This means that there is a*
 161 *need to scale the permeability from the capillary tube model to include increased path length due to crookedness of the path*
 162 *(tortuosity) or lack of connection between points in the soil (connectivity)*”. Soils that are poorly connected and have highly
 163 crooked pathways theoretically have τ_1 , τ_2 , $\tau_3 \approx 0.9$. Further explanation of tortuosity is provided in Table 2.

164
 165 **Table 2. Please insert here**

166 2.3. Romano bimodal water retention curve

167 New Zealand soils are predominantly well structured, with two-stage drainage (Carrick et al., 2010; McLeod et al., 2008),
 168 and therefore have a bimodal pore-size distribution (e.g. Durner, 1994). As K_{s_umi} is based on a unimodal curve, $\theta_{umi}(h)$, the
 169 proposed bimodal model, K_{s_bim} , should be based on a bimodal $\theta_{bim}(h)$ curve.

170
 171 Borgesen et al. (2006) showed that structured soils have both *matrix* (inter-aggregate) pore spaces and *macropore*
 172 (intra-aggregate) pore spaces. Thus, when the pores are initially saturated ($r > R_{mac}$) or ($h < H_{mac}$), the flow is considered
 173 *macropore* flow, and when the soil is desaturated ($r < R_{mac}$) or ($h > H_{mac}$), the flow is considered *matrix* flow, as shown in

174 Fig. 1. R_{mac} is the theoretical pore size r that delimits macropore and matrix flow and H_{mac} is the theoretical pressure that
 175 delimits macropore and matrix flow. To model bimodal pore-size distribution Durner (1994) superposes two unimodal
 176 pore-size distributions by using an empirical weighting factor, W , which partitions the volumetric percentage of macropore
 177 and matrix pores. Recently Romano et al. (2011) proposed the following Kosugi bimodal $\theta_{\text{bim_rom}}(h)$ distribution:

$$178 \quad \theta_{\text{bim_rom}}(h) = (\theta_s - \theta_r) \left\{ W \operatorname{erfc} \left[\frac{\ln h - \ln h_{m_mac}}{\sigma_{mac} \sqrt{2}} \right] + (1 - W) \operatorname{erfc} \left[\frac{\ln h - \ln h_m}{\sigma \sqrt{2}} \right] \right\} + \theta_r \quad (9)$$

179 where θ_s , ~~$\ln(h_{m_mac})$~~ and σ_{mac} are, respectively, the *saturated water content*, the *median pore radius*~~es~~ and the *standard*
 180 *deviation* of $\ln(h)$ of the macropore domain, θ_r , h_m and σ are parameters of the matrix domain, and W is a constant in the
 181 range $[0,1)$.

182 3 Theoretical development of novel bimodal saturated hydraulic conductivity

183 We report on further adaptations to the physical model of Pollacco et al. (2013) to suit it to dual-porosity structured soils,
 184 which are common in New Zealand, solely from Kosugi hydraulic parameters describing $\theta(h)$. This involves:

- 185 • rewriting the Romano bimodal $\theta(h)$ (Sec. 3.1),
- 186 • developing a novel bimodal K_s model based on the modified bimodal $\theta(h)$ (Sec. 3.2).

187 3.1 Modified Romano bimodal water retention curve

188 We propose a modified version of $\theta_{\text{bim_rom}}(h)$ (Eq. (9)) that does not use the empirical parameter W . Our modified function,
 189 $\theta_{\text{bim}}(h)$, is plotted in Fig. 1 and is computed as:

$$191 \quad \theta_{\text{bim}}(h) = \theta_{\text{bim_mat}}(h) + \theta_{\text{bim_mac}}(h) \quad (10a)$$

$$192 \quad \theta_{\text{bim_mat}}(h) = [\theta_{s_mac} - \theta_r] \operatorname{erfc} \left[\frac{\ln h - \ln h_m}{\sigma \sqrt{2}} \right] + \theta_r \quad (10b)$$

$$193 \quad \theta_{\text{bim_mac}}(h) = [\theta_s - \theta_{s_mac}] \operatorname{erfc} \left[\frac{\ln h - \ln h_{m_mac}}{\sigma_{mac} \sqrt{2}} \right] \quad (10c)$$

194 where θ_{s_mac} is the *saturated water content* that theoretically differentiates *macropore* and *matrix* domains.

196 The shape of $\theta_{\text{bim}}(h)$ is identical to that of $\theta_{\text{bim_rom}}(h)$, but the advantage of $\theta_{\text{bim}}(h)$ is that it uses the physical parameter
 197 θ_{s_mac} instead of the empirical parameter W , and θ_{s_mac} ($\leq \theta_s$) is more easily parameterized than W particularly when there is
 198 no available data in the macropore domain. When we do not have data in the macropore domain, θ_{s_mac} is determined by
 199 fitting the hydraulic parameters θ_{s_mac} , θ_r , h_m , σ of $\theta_{\text{bim_mat}}(h)$ (Eq. (10b)) solely in the matrix range ($r < R_{\text{mac}}$ or $h > H_{\text{mac}}$) by
 200 ensuring that $\theta_{s_mac} \leftarrow \theta_r$. Fig. 1 shows that R_{mac} and θ_{s_mac} delimit the matrix and the macropore domains and that r_m of the
 201 Kosugi model is the inflection point of $\theta_{\text{bim_mat}}(h)$ and r_{m_mac} is the inflection point of $\theta_{\text{bim_mac}}(h)$.

202
203

Fig. 1. Please put it here

204 **3.2 Novel bimodal saturated hydraulic conductivity model**

205 Using $\theta_{\text{bim}}(h)$, we propose a new bimodal $K_{s,\text{bim}}(S_e)$ that is derived following $K_{s,\text{uni}}(S_e)$ (Eq. (7)) but for which we add a
 206 macropore domain:

207
$$K_{s,\text{bim}} = K_{s,\text{bim},\text{mat}} + K_{s,\text{bim},\text{mac}} \quad (11a)$$

208
$$K_{s,\text{bim},\text{mat}} = C \int_0^1 (1 - \tau_1) (\theta_{s,\text{mac}} - \theta_r)^{\frac{1}{1-\tau_3}} (r_{\text{matrix}})^{2(1-\tau_2)} dS_e \quad (11b)$$

209
$$K_{s,\text{bim},\text{mac}} = C \int_0^1 (1 - \tau_{1,\text{mac}}) (\theta_s - \theta_{s,\text{mac}})^{\frac{1}{1-\tau_{3,\text{mac}}}} (r_{\text{macropore}})^{2(1-\tau_{2,\text{mac}})} dS_e \quad (11c)$$

210 where $r_{\text{macropore}}$ is $r \geq R_{\text{mac}}$ and r_{matrix} is $r < R_{\text{mac}}$.

211 The r_{matrix} of Eq. (11b) is derived from Eq. (2b):

212
$$r_{\text{matrix}} = \frac{r_m}{\exp\left[\text{erfc}^{-1}\left[2 S_e\right] \sigma \sqrt{2}\right]} \quad (12)$$

213 and $r_{\text{macropore}}$ is computed similarly as:

214
$$r_{\text{macropore}} = \frac{r_{m,\text{mac}}}{\exp\left[\text{erfc}^{-1}\left[2 S_e\right] \sigma_{\text{mac}} \sqrt{2}\right]} \quad (13)$$

215

216 We introduced r_{matrix} (Eq. (12)) and $r_{\text{macropore}}$ (Eq. (13)) into $K_{s,\text{bim}}$ (Eq. (11a)), giving the equation for $K_{s,\text{bim}}$:

217
$$K_{s,\text{bim}} = C \int_0^1 \left[(1 - \tau_1) (\theta_{s,\text{mac}} - \theta_r)^{\frac{1}{1-\tau_3}} \left\{ \frac{r_m}{\exp\left[\text{erfc}^{-1}\left[2 S_e\right] \sigma \sqrt{2}\right]} \right\}^{2(1-\tau_2)} + \right. \\ \left. (1 - \tau_{1,\text{mac}}) (\theta_s - \theta_{s,\text{mac}})^{\frac{1}{1-\tau_{3,\text{mac}}}} \left\{ \frac{r_{m,\text{mac}}}{\exp\left[\text{erfc}^{-1}\left[2 S_e\right] \sigma_{\text{mac}} \sqrt{2}\right]} \right\}^{2(1-\tau_{2,\text{mac}})} \right] dS_e \quad (14a)$$

218 or

219
$$K_{s,\text{bim}} = C \int_0^1 \left[(1 - \tau_1) (\theta_{s,\text{mac}} - \theta_r)^{\frac{1}{1-\tau_3}} \left\{ \frac{Y}{h_m} \right\}^{2(1-\tau_2)} \exp\left[\text{erfc}^{-1}\left(2 S_e\right) \sigma \sqrt{2}\right] + \right. \\ \left. (1 - \tau_{1,\text{mac}}) (\theta_s - \theta_{s,\text{mac}})^{\frac{1}{1-\tau_{3,\text{mac}}}} \left\{ \frac{Y}{h_{m,\text{mac}}} \right\}^{2(1-\tau_{2,\text{mac}})} \exp\left[\text{erfc}^{-1}\left(2 S_e\right) \sigma_{\text{mac}} \sqrt{2}\right] \right] dS_e \quad (14b)$$

220

221 In Eq. (14b), $r_{m,\text{mac}}$ is replaced by $Y/h_{m,\text{mac}}$ and r_m is replaced by Y/h_m and for the computation of K_s , than $K_{s,\text{bim}}(S_e=1)$. Note
 222 that the bimodal K_s model requires that the flow in the macropore domain obeys the Buckingham–Darcy law. Therefore, this

223 model's performance may be restricted in cases of non-Darcy flow, such as non-laminar and turbulent flow, which may
224 occur in large macropores.

225
226 In this study σ_{mac} is not derived from measured $\theta(h)$ because measured data in the macropore domain are ~~difficult to~~
227 ~~find~~not always available, and so it will be treated as a fitting parameter. As discussed above, θ_{s_mac} , θ_r , σ and h_m are
228 optimized with $\theta_{uni}(h)$ measurement points only in the matrix range ($r < R_{mac}$ or $h > H_{mac}$), which means that θ_s is not
229 included in the observation data. In summary, K_{s_bim} requires optimization of the parameters τ_1 , τ_2 , τ_3 , and τ_{1_mac} , τ_{2_mac} , τ_{3_mac}
230 and h_{m_mac} , σ_{mac} (if no data are available in the macropore domain). The theoretically feasible range of the parameters of
231 K_{s_bim} is shown in Table 3.

232 **Table 3. Please put table here.**

233
234 One of the limitations of the New Zealand data set is that it has no $\theta(h)$ data points in the macropore domain. The
235 closest data point near saturation is $\theta(h = 50 \text{ cm})$, which is in the matrix pore space. Carrick et al. (2010) found that H_{mac}
236 ranges from 5 to 15 cm, with an average $H_{mac} = 10 \text{ cm}$, which corresponds to a circular pore radius of $R_{mac} = 0.0149 \text{ cm}$ (e.g.
237 Jarvis, 2007; Jarvis and Messing, 1995; Messing and Jarvis, 1993). Therefore, to reduce the number of optimized parameters
238 we make the following assumption:

239
$$h_{m_mac} = \exp \left[\frac{\ln(H_{mac})}{P_{m_mac}} \right] \quad (15)$$

240 where P_{m_mac} is a fitting parameter greater than 1. We found the fitted value of P_{m_mac} was 2.0, however this fitted parameter
241 was very broadly determined. The cause might be that we are optimizing σ_{mac} and therefore h_{m_mac} and σ_{mac} might be linked.
242 Linked parameters (Pollacco et al., 2008a, 2008b, 2009) means that there is an infinite combination of sets of linked
243 parameters h_{m_mac} and σ_{mac} which produces values of objective function close to that obtained with the optimal parameter set
244 and for which there exists a continuous relationship between h_{m_mac} and σ_{mac} . Further research needs to determine if having
245 more data in the macropore domain would reduce the cause of non-uniqueness. To illustrate h_{m_mac} this, the equivalent r_{m_mac}
246 (H_{m_mac}) point is shown in Fig. 1, where r_{m_mac} is the inflection point of the macropore domain. Fig. 1 also shows that the
247 matrix and the macropore domains meet at $R_{mac} (H_{mac})$.

248 **4 Methods**

249 **4.1 Data**

250 **4.1. Measurement of physical soil properties & Selecting soil samples from New Zealand Soils Database**

251 The soils data used in this study were sourced from two data sets. In the first data set (Canterbury Regional Study;
252 Table 4) soils were derived from eight soils series on the post-glacial and glacial alluvial fan surfaces of the Canterbury
253 Plains (Webb et al., 2000). The soils varied from shallow, well-drained silt loam soils to deep, poorly drained clay loam
254 soils. The second data set was derived from the Soil Water Assessment and Measurement Programme to physically
255 characterize key soils throughout New Zealand in the 1980s. Soils selected from this data set are listed by region in Table 4
256 and were selected from soils formed from sediments derived from indurated sandstone rocks, because this is the most
257 common parent material for soils in New Zealand and has a reasonably representative number of soils analysed for physical
258 properties.

259
260
261
262
263
264
265
266
267
268
269
270
271
272
273
274
275
276
277
278
279
280
281
282
283
284
285
286
287
288
289
290
291
292
293
294
295
296
297
298

The cores for particle size analysis and measurement of $\theta(h)$ had diameters which ranges from 5.5 cm to 10 cm diameter and having height which varied from 5 to 6 cm. The 5, 10 kPa measurements of the $\theta(h)$ were derived using the suction table method as per Dane and Topp, (2002) following the NZ Soil Bureau laboratory method (Gradwell, 1972). For the 20 to 1500 kPa of the $\theta(h)$ were measured using pressure plate method as per Dane and Topp, (2002), following the NZ Soil Bureau method (Gradwell, 1972). The

Laboratory analysis for particle size followed Gradwell (1972).

The total porosity, ϕ , described in Eq. (5) contains uncertainties from the measurement methods, where ϕ is derived from separate measurements of particle density and bulk density, rather than being directly measured. The uncertainty in ϕ measurements appeared to have reduced the demonstrated benefits of using K_{s_bim} instead of K_{s_uni} , which strongly relies on $\phi \alpha - \theta_{mac}$ and may have caused the optimal α to be 0.98 and not the commonly accepted value of 0.95 (Rogowski, 1971; Pollacco et al., 2013; Haverkamp et al., 2005; Leij et al., 2005).

The 5, 10 kPa of the $\theta(h)$ were derived using suction table method as per Dane and Topp, (2002) following the NZ Soil Bureau laboratory method (Gradwell, 1972). For the 20 to 1500 kPa of the $\theta(h)$ were measured using pressure plate method as per Dane and Topp, (2002), following NZ soil Bureau method (Gradwell, 1972).

~~The soils data used in this study were sourced from two data sets. The first data set (Canterbury Regional Study; Table 4) soils were derived from eight soils series on the post glacial and glacial surfaces of the Canterbury Plains (Webb et al., 2000). The soils varied from shallow, well drained silt loam soils to deep, poorly drained clay loam soils. The second data set was derived from the Soil Water Assessment and Measurement Programme to physically characterize key soils throughout New Zealand in the 1980s. Soils selected from this data set are listed by region in Table 4. All soils selected were from soils formed from sediments derived from indurated sandstone rocks, because this is the most common parent material for soils in New Zealand and has a reasonably representative number of soils analysed for physical properties. Each soil series had nine profiles. Three horizons in each soil profile were sampled from deep soils (topsoil, horizon with slowest permeability, and the main horizon between these) and two from shallow soils (topsoil and the main horizon above gravels). Grab samples were taken for particle size analysis, a 5.5 cm diameter core was taken from the middle of each horizon for moisture release analysis, and three 10 cm diameter cores were taken from the upper part of each horizon for hydraulic conductivity analysis.~~

~~The second data set was derived from the Soil Water Assessment and Measurement Programme to physically characterize key soils throughout New Zealand in the 1980s. Soils selected from this data set are listed by region in Table 4. All soils selected were from soils formed from sediments derived from indurated sandstone rocks, because this is the most common parent material for soils in New Zealand and has a reasonably representative number of soils analysed for physical properties. Selection of horizons and core size was similar to the Canterbury regional study, except that more subsoil horizons were sampled at some sites, cores for hydraulic conductivity were not sampled in the topsoil horizon, and four to six cores for hydraulic conductivity were sampled in subsoils.~~

~~4.1.2 Measuring water retention curves and total porosity~~

~~Laboratory analysis for particle size followed Gradwell (1972). The soil moisture retention curves were derived by using 5.5 cm diameter cores according to the methods of Gradwell (1972).~~

299
300
301
302
303
304
305
306
307
308
309
310
311
312
313
314
315
316
317
318
319
320
321
322
323
324
325
326
327
328
329
330
331
332
333
334
335
336

~~The total porosity, ϕ , described in Eq. (5) contains uncertainties from the measurement methods, where ϕ is derived from separate measurements of particle density and bulk density, rather than being directly measured. The uncertainty in ϕ measurements appeared to have reduced the demonstrated benefits of using K_{s_min} instead of K_{s_mac} , which strongly relies on $\phi \propto \theta_{s_mac}$ and may have caused the optimal α to be 0.98 and not the commonly accepted value of 0.95 (Rogowski, 1971; Pollacco et al., 2013; Haverkamp et al., 2005; Leij et al., 2005).~~

Table 4. Please put here

4.1.3 Measuring saturated hydraulic conductivity performed with problematic small cores

The K_s data used were collected and processed at a time when the best field practices in New Zealand were still being explored. K_s was derived using constant-head Mariotte devices (1 cm head) from three to six cores (10 cm diameter and 7.5 cm thickness) for each horizon. The \log_{10} scale value of the standard error of the replicates of the measurements is shown in Fig. 2, which shows large uncertainty in the measurements (up to three orders of magnitude). This uncertainty is due to:

- a) **measurements of $\theta(h)$ and K_s being taken on different cores**, which caused some mismatch between $\theta(h)$ and K_s , resulting in 16 outliers that negatively influenced the overall fit of the K_s model having to be removed from the data set
- b) **side leakage** of some cores, which led to K_s values that were too high (Carrick, 2009), resulting in six samples with unusually high K_s having to be removed from the data set
- c) **misreporting low K_s** since the measurements of K_s were halted when conductivity was less than 0.1 cm day^{-1} , resulting in four samples with low K_s having to be removed from the data set
- d) **small core samples**, which led to considerable variability in the absence/presence of structured cracks caused by roots or worm burrows (McKenzie and Cresswell, 2002; Anderson and Bouma, 1973) that were evident in dyed samples; we therefore removed measured K_s replicates that were too high and showed evidence of macropore abundance by having values of $\theta_s - \theta_{s_mac} > 0.05$.

We therefore selected 235/262 samples (90%) and removed only 27 outliers, which is minimal compared, for instance, to the UNSODA (Leij et al., 1999; Schaap and van Genuchten, 2006) and HYPRES databases (Wösten et al., 1998; Wösten et al., 1999; Lilly et al., 2008), which are used for the development of PTFs such as the ROSETTA PTF (Patil and Rajput, 2009; Rubio, 2008; Young, 2009), and which were found to contain a large number of outliers. Using these databases, Pollacco et al. (2013) selected only 73/318 soils (23%), which complied with strict selection criteria prior to modelling.

Note that the K_s observations in the topsoils have greater variability than in the subsoil layers (Fig. 2). This is because topsoils are more disturbed by ~~anthropogenic disturbance and biological activity, tillage, planar fissures formed by wetting/drying, compaction, growth of plant roots and earthworm burrowing~~. Therefore, the topsoils also have a greater abundance of macropores, and therefore are more prone to error when the sampling is performed with a small core size that does not contain a representative volume of the macropore network.

Fig. 2. Please insert figure here

4.2 Inverse modelling and goodness of fit

The parameterization of the model was performed in two consecutive steps:

1. Optimization of θ_{s_mac} , θ_r , h_m and σ of the unimodal Kosugi $\theta_{bim_mat}(h)$ (Eq. (4.10b)) was performed by matching observed and simulated $\theta(h)$ in the range $h < H_{mac}$ (as discussed, θ_s is not included in the observation data since we did not have data in the macropore domain). The feasible ranges of the Kosugi parameters are described in Table 1.
2. Optimization of the τ_1 , τ_2 , τ_3 of the K_{s_uni} model (Eq. (8)) and τ_{1_mac} , τ_{2_mac} , τ_{3_mac} , σ_{mac} parameters of the K_{s_bim} models (Eq. (14)), where the physical feasible ranges of the tortuosity parameters are described in Table 3.

The inverse modelling was performed in MATLAB using AMALGAM in MATLAB, which is a robust global optimization algorithm (<http://faculty.sites.uci.edu/jasper/sample/>) (e.g., ter Braak and Vrugt, 2008). For each step we minimized the objective functions described below.

4.2.1 Inverting the Kosugi hydraulic parameters

The objective function, OF_θ , used to parameterize Kosugi's $\theta(h)$ at the following pressure points [5, 10, 20, 40, 50, 100, 1500 kPa], is described by:

$$OF_\theta = \sum_{i=1}^{i=N_\theta} [\theta_{sim}(h_i, \mathbf{p}_\theta) - \theta_{obs}(h_i)]^{P_{over}} \quad (16)$$

where the subscripts *sim* and *obs* are simulated and observed, respectively. \mathbf{P}_θ is the set of predicted parameters (θ_{s_mac} , θ_r , h_m , σ) and P_{over} is the power of the objective function.

The computation of K_{s_bim} requires $\theta(h)$ to be accurate near saturation, when the drainage is mostly from large pores, and to achieve this balance we found by trial and error that best results are achieved when we make P_{over} large (equal to 6).

4.2.2 Calibrating the tortuosity parameters of the saturated hydraulic conductivity model

The parameters of K_{s_uni} and K_{s_bim} models were optimized by minimizing the following objective function OF_{ks} :

$$OF_{ks} = \sum_{j=1}^{j=N_{ks}} [\ln K_{s_sim}(\mathbf{p}_{ks}) - \ln K_{s_obs}]^2 \quad (17)$$

where the subscripts *sim* and *obs* are simulated and observed, respectively. \mathbf{P}_{ks} is the vector of the unknown parameters. The log transformation of OF_{ks} puts more emphasis on the lower K_{obs} and therefore reduces the bias towards larger conductivity (e.g. van Genuchten et al., 1991; Pollacco et al., 2011). Also, the log transformation considers that the uncertainty in measured unsaturated hydraulic conductivity increases as $K(\theta)$ increases.

The goodness of fit between simulated (K_{s_uni} or K_{s_bim}) and observed K_s was computed by the $RMSE_{\log_{10}}$:

$$RMSE_{\log_{10}} = \sqrt{\frac{\sum_{j=1}^{j=N_{ks}} [\log_{10} K_{s_sim} - \log_{10} K_{s_obs}]^2}{N}} \quad (18)$$

where N is the number of data points.

368 The following transformation was necessary to scale the parameters to enable the global optimization to converge to a
 369 solution:

$$370 \quad \tau_1 = 1 - 10^{-T_1} \quad (19)$$

371 where T_1 is a transformed tortuosity τ_1 .

372

373 Introducing Eq. (19) into K_{s_bim} Eq. (14) gives:

$$374 \quad K_{s_bim} = C \int_0^1 \left[10^{-T_1} (\theta_{s_mac} - \theta_r)^{\frac{1}{1-\tau_3}} \left\{ \frac{\frac{Y}{h_m}}{\exp \left[\operatorname{erfc}^{-1}(2 S_e) \sigma \sqrt{2} \right]} \right\}^{2(1-\tau_2)} + \right. \\ \left. 10^{-T_{1_mac}} (\theta_s - \theta_{s_mac})^{\frac{1}{1-\tau_{3_mac}}} \left\{ \frac{\frac{Y}{h_{m_mac}}}{\exp \left[\operatorname{erfc}^{-1}(2 S_e) \sigma_{_mac} \sqrt{2} \right]} \right\}^{2(1-\tau_{2_mac})} \right] dS_e \quad (20)$$

375

376 5 Results and discussion

377 We report on (1) the suitability of the K_{s_uni} model (developed with European and American data sets, Pollacco et al., 2013)
 378 to predict K_s for New Zealand soils experiencing large uncertainties, as shown in Fig. 2; (2) improvements made by
 379 stratifying the data with texture and topsoil/subsoil; and (3) ~~enhancements improvements~~ made by using the bimodal K_{s_bim}
 380 instead of the unimodal K_{s_uni} .

381 5.1 Improvement made by stratifying with texture and topsoil/subsoil

382 It was expected that stratifying with texture and topsoil/subsoil (layers) should improve the predictions of K_s to only a
 383 modest degree. This is because K_{s_bim} and K_{s_uni} are physically based models that are based on pore-size distribution, and
 384 therefore stratifying with soil texture or topsoil/subsoil are not likely to provide extra information. For instance, Arya and
 385 Paris (1981) showed that there is a strong relationship between pore-size distribution and the particle-size distribution and
 386 therefore adding soil texture information should not improve the model.

387 **Table 5. please put table here**

388 ~~As expected~~, no significant improvements were made by stratifying with soil texture compared with a model that
 389 groups all texture classes (loam and clay) and layers (topsoil and subsoil) (overall improvement of 3%) (Table 5). However,
 390 a significant improvement was made by stratifying by layer (topsoil and subsoil) (overall improvement of 23%), and
 391 therefore the remaining results are presented by stratifying by layer. These results are obtained because topsoils have higher
 392 macropores and a smaller tortuous path than that in subsoil, as demonstrated by $\tau_{1_top} > \tau_{1_sub}$ or $T_{1_top} < T_{1_sub}$, $\tau_{2_top} > \tau_{2_sub}$,
 393 $\tau_{3_top} > \tau_{3_sub}$ (Table 6). It is important to note that tortuosity decreases as τ becomes closer to 1.

394 **Table 6. Please put table here**

395 5.2 Improvement made by using K_{s_bim} instead of K_{s_uni}

396 Figure 3 shows an acceptable fit between K_{s_bim} and K_{s_obs} (RMSElog₁₀ = 0.450 cm day⁻¹), recognizing that the observations
 397 contain large uncertainties since the measurements were taken by using small cores (Sect. 4.1.3). The overall improvement

398 made by using K_{s_bim} is somewhat modest (5% for all soils). As expected, the reasonable improvement is greater for topsoil
399 containing higher macroporosity (12% improvement) than for subsoil (4% improvement) (Table 6). This is because topsoil
400 has higher macropore θ_{mac} ($\theta_s - \theta_{s_mac}$) (Table 7) caused by earthworm channels, fissures, roots and tillage than subsoil.

401

402 The RMSElog₁₀ of K_{s_uni} for subsoil is 0.47 cm day⁻¹ (Table 6) which is slightly worse compared to the RMSElog₁₀ of
403 0.420 cm day⁻¹ by using UNSODA and HYPRES data sets (Pollacco et al., 2013).

404

405 **Table 7. Please put table here**

406

407

408 The reason K_{s_bim} shows smaller-than-expected improvements compared to K_{s_uni} requires further investigation and
409 testing with a data set containing fewer uncertainties. One plausible explanation is that K_{s_bim} is highly sensitive to θ_s ,
410 computed from total porosity ϕ (Eq. (6)), which had inherent measurement uncertainties (Sect. 4.1.2). In addition, the
411 possible existence of non-Darcy flow in large biological pores may decrease the outperformance of the bimodal model over
412 the unimodal model.

413

Fig. 3. Please insert Figure 3 here

414 **5.2.3 Optimal tortuosity parameters**

415 The optimal tortuosity parameters of K_{s_bim} and K_{s_uni} (Table 6) show that the optimal parameters are within the physically
416 feasible limits, except for τ_{3_mac} of the subsoil, which are greater than τ_3 . This is understandable because Pollacco et al.
417 (2013) found τ_3 not to be a very sensitive parameter. As expected, T_{1_mac} is smaller than T_1 ($\tau_{1_mac} > \tau_1$), which suggests that
418 the tortuosity parameters have a physical meaning.

419

420 The estimated value of the unimodal T_1 parameter K_{s_uni} derived from the UNSODA and HYPRES data sets ($T_1 = 0.1$)
421 (Pollacco et al., 2013) is very different from the value estimated in this present study ($T_1 = 6.5$). Cichota et al. (2013) also
422 reported that PTFs developed in Europe and the USA were not applicable to New Zealand. The reasons why these PTFs are
423 not directly applicable to New Zealand require further investigation.

424 **5.3.4 Uncertainty of the bimodal saturated hydraulic conductivity model predictions**

425 The practical application of the bimodal saturated hydraulic conductivity model, K_{s_bim} , to New Zealand soils requires a
426 model for the uncertainty of the resultant predictions, since it is then possible to attach a value for the uncertainty of future
427 predictions of K_s . In a conventional parametric statistical model, the uncertainty model follows from the structure of the
428 fitting model itself. In the present work, K_s is estimated using an inverse model and this has no associated functional
429 uncertainty model. For this reason, the uncertainty is derived empirically by fitting a relationship between the transformed
430 residuals of the model (the log-transformed measured K_s minus the log-transformed estimated K_s) as a function of the
431 log-transformed estimated K_s . Although the uncertainty model could be derived from all the soils in the study, this process
432 results in a pooled estimate for uncertainty (e.g., aggregated root mean square error). However, it has been observed that
433 topsoils and subsoils have different uncertainty behaviour for the estimated K_s , so it is desirable to include an indicator
434 variable to determine whether the soil is a topsoil or not. In explicit form,

$$435 \log_{10} K_{s_obs} - \log_{10} K_{s_sim} = a_1 L + a_0 + \epsilon \quad (21)$$

436 where a_0 and a_1 are fitting constants, L is an indicator variable specifying whether the soil is a topsoil (value 1), or a
437 subsoil (value 0), and ϵ is the uncertainty distribution. The distribution of the uncertainty ϵ could take a number of forms,
438 but there is no obvious choice, except that one might expect the distribution central measure to be unbiased. To avoid an
439 explicit distribution assumption, we fitted a conditional quantile model (Koenker, 2005) for the transformed residuals, based
440 on the τ quantile, where $\tau = 0.5$ corresponds to the conditional median, and $\tau = 0.025$ and $\tau = 0.975$ correspond
441 respectively to the 2.5% and 97.5% quantiles, and thus together describe the 95% containment interval of the residuals.

442 The conditional quantile model Eq. (21) was fitted using $\tau = 0.5, 0.025$ and 0.975 (Table 8). The results suggest a
443 strong dependence of the scale of the residuals on whether the soil is a topsoil or not, but the size of the 95% residual
444 containment interval is not dependent on the simulated K_s . Notably, the confidence interval for the fitted median ($\tau = 0.5$)
445 quantile model suggests that the uncertainty distribution median is unbiased; thus predictions from K_{s_bim} show no propensity
446 for bias, which is a desirable result.

447 **Table 8. Please put here**

448 Another way to illustrate the uncertainty model is to plot the observed $\log_{10} K_{s_obs}$ against the estimated $\log K_{s_bim}$,
449 with the fitted median, lower and upper 95% quantile lines, as shown in Fig. 4. The width of the 95% containment interval
450 for the residuals is narrower (i.e., the predictions appear to be more accurate) for topsoils. The quantile estimates for the
451 conditional median of both topsoil and subsoil are also shown in Fig. 4, with the shaded region showing the 95% confidence
452 interval of the median estimate. The shaded region covers the one-to-one line in Fig. 4, and thus there is no compelling
453 evidence that the median residual distribution is biased.

454 **Fig. 4. Please put here**

455 **5.4.6 Recommended future work to improve the New Zealand soil database**

456 A key outcome of this research will be to provide direction for future field studies to quantify soil water movement attributes
457 of New Zealand soils, and to prioritise which measurements will have the greatest value to reduce the uncertainty in
458 modelling of the soil moisture retention and hydraulic conductivity relationships. Recommendations are:

- 459 • Evaluate the spatial representativeness of the current soil physics data set and undertake more measurements of
460 hydraulic conductivity and soil water retention on key soils.
- 461 • Use larger cores for measurements of hydraulic conductivity.
- 462 • Take measurements of the moisture retention curve and saturated hydraulic conductivity on the same sample.
- 463 • Provide more accurate measurements of total porosity.
- 464 • Conduct near saturation measurements of $\theta(h)$ and $K(\theta)$ to better characterize the macropore domain, which is
465 responsible for preferential flow behaviour.
- 466 • Make more accurate measurements on slowly permeable soils ($< 1 \text{ cm day}^{-1}$), which are important for management
467 purposes but are not well represented in the current databases.

468 **7 Conclusions**

469 We report here on further adaptations to the saturated hydraulic conductivity unimodel to suit it to dual-porosity- structured
470 soils (Eq. 10)-by computing the soil water flux through a continuous function of a modified version of a improved-Romano
471 et al. (2011) $\theta(h)$ dual pore-size distribution (Eq. 18). The shape of the improved-Romano $\theta(h)$ distribution is identical to the

472 | ~~modified improved~~ $\theta(h)$, but the advantage of the developed bimodal $\theta(h)$ is that it is more easily parameterized when no
473 data are available in the macropore domain.

474

475 The stratification of the data with texture only (loam or clay) slightly improved the predictions of the K_s model, which
476 is based on pore-size distribution. This gives us confidence that the K_s model is accounting for the effect of these physical
477 parameters on K_s . A significant improvement was made by separating topsoils from subsoils. The improvements are higher
478 for the topsoil, which has higher macroporosity caused by roots and tillage compared to subsoils. The reason why a model
479 with no stratification is not sufficient is unclear and requires further investigation.

480

481 The improvements made by using the developed bimodal K_{s_bim} (Eq. 1820) compared to the unimodal K_{s_uni} (Eq. 8) is
482 modest overall, but, as expected, greater for topsoils having larger macroporosity. Nevertheless, an acceptable fit between
483 K_{s_bim} with K_{s_obs} was obtained when due recognition was given to the high variability in the measured data. We expect K_{s_bim}
484 to provide greater improvement in K_s predictions if more $\theta(h)$ measurements are made at tensions near saturation and if
485 measurements are made on larger cores and with more accurate measurements of porosity.

486

487 Data availability

488 The data are part of the New Zealand soil databases, available at <http://smap.landcareresearch.co.nz/> and
489 <https://soils.landcareresearch.co.nz/>.

Field Code Changed

490 Acknowledgements

491 We are grateful to Leah Kearns and for Ray Prebble, who improved the readability of the manuscript and for anonymous
492 reviewers 1 & 3 who significantly improved the clarity of the manuscript. This project was funded by Landcare Research
493 core funding, through the New Zealand Ministry of Business, Innovation and Employment.

494

Comment [McNeill1]: Why exclude reviewer 2? Better to thank all of them and move on...

495 References

- 496 [Anon: The History of Poiseuille's Law. Annual Review of Fluid Mechanics, 25\(1\), 1–20, doi:10.1146/annurev.fl.25.010193.000245.1993.](#)
497
498 Anderson, J. L., and Bouma, J.: Relationships between saturated hydraulic conductivity and morphometric data of an argillic
499 horizon1, Soil Sci. Soc. Am. J., 37, 408–413, doi:10.2136/sssaj1973.03615995003700030029x, 1973b.
500 Arya, L. M., and Paris, J. F.: A physicoempirical model to predict the soil moisture characteristic from particle-size
501 distribution and bulk density data, Soil Science Society of America Journal, 45, 1023–1030,
502 doi:10.2136/sssaj1981.03615995004500060004x, 1981.
503 Balland, V., and Pollacco, J. A. P.: Modeling soil hydraulic properties for a wide range of soil conditions, Ecological
504 Modelling, 219, 300–316, 2008.
505 Borgesen, C. D., Jacobsen, O. H., Hansen, S., and Schaap, M. G.: Soil hydraulic properties near saturation, an improved
506 conductivity model, Journal of Hydrology, 324, 40–50, doi:10.1016/j.jhydrol.2005.09.014, 2006.
507 Brooks, R. H., and Corey, A. T.: Hydraulic properties of porous media, Hydrol. Pap., 3, 1964.
508 Carrick, S.: The dynamic interplay of mechanisms governing infiltration into structured and layered soil columns, PhD,
509 Lincoln University, Lincoln, 2009.
510 Carrick, S., Almond, P., Buchan, G., and Smith, N.: In situ characterization of hydraulic conductivities of individual soil
511 profile layers during infiltration over long time periods, European Journal of Soil Science, 61, 1056–1069,
512 doi:10.1111/j.1365-2389.2010.01271.x, 2010.

- 513 Carrick, S., Buchan, G., Almond, P., and Smith, N.: Atypical early-time infiltration into a structured soil near field capacity:
514 the dynamic interplay between sorptivity, hydrophobicity, and air encapsulation, *Geoderma*, 160(3–4), 579–589,
515 doi:10.1016/j.geoderma.2010.11.006, 2011.
- 516 [Chapuis, R. P.: Predicting the saturated hydraulic conductivity of sand and gravel using effective diameter and void ratio,
517 *Can. Geotech. J.*, 41\(5\), 787–795, doi:10.1139/t04-022, 2004.](#)
- 518 Childs, E. C., and Collisgeorge, N.: The permeability of porous materials, *Proc. R. Soc. Lon. Ser-A*, 201, 392-405,
519 doi:10.1098/rspa.1950.0068, 1950.
- 520 Cichota, R., Vogeler, I., Snow, V. O., and Webb, T. H.: Ensemble pedotransfer functions to derive hydraulic properties for
521 New Zealand soils, *Soil Research*, 51, 94–111, doi:10.1071/sr12338, 2013.
- 522 [Cox, S. C., and Barrell D. J. A.: *Geology of the Aoraki Area. Institute of Geological & Nuclear Sciences 1:250 000 map 15-
523 1 sheet +71 p. Lower Hutt, New Zealand. Institute of Geological & Nuclear Sciences, 2007.*](#)
- 524 [Dane, J.H., and Topp, G. C.: *Methods of Soil Analysis, Part 4. Physical Methods. Soil Science Society of America Book
525 Series No. 5. Madison, WI, USA Pages 692-698, 2002*](#)
- 526 Durner, W.: Hydraulic conductivity estimation for soils with heterogeneous pore structure, *Water Resources Research*, 30,
527 211–223, doi:10.1029/93wr02676, 1994.
- 528 Fatt, I., and Dykstra, H.: Relative permeability studies, *T. Am. I. Min. Met. Eng.*, 192, 249–256, 1951.
- 529 [Forsyth, P. J., Barrell, D. J. A. and Jongens, R.: *Geology of the Christchurch Area. Institute of Geological & Nuclear
530 Sciences 1:250 000 map 16. 1 sheet +67 p. Lower Hutt, New Zealand. Institute of Geological & Nuclear Sciences,
531 2008.*](#)
- 532 Gradwell, M. W.: Methods for physical analysis of soils. In *New Zealand Soil Bureau Scientific Report No. 10C*, 1972.
- 533 Griffiths, E., Webb, T. H., Watt, J. P. C., and Singleton, P. L.: Development of soil morphological descriptors to improve
534 field estimation of hydraulic conductivity, *Australian Journal of Soil Research*, 37, 971–982, doi:10.1071/sr98066,
535 1999.
- 536 Haverkamp, R., Leij, F. J., Fuentes, C., Sciortino, A., and Ross, P. J.: Soil water retention: I. Introduction of a shape index,
537 *Soil Science Society of America Journal*, 69, 1881–1890, doi:10.2136/sssaj2004.0225, 2005.
- 538 Hayashi, Y., Kosugi, K., and Mizuyama, T.: Soil water retention curves characterization of a natural forested hillslope using
539 a scaling technique based on a lognormal pore-size distribution, *Soil Science Society of America Journal*, 73, 55–64,
540 2009.
- 541 Jarvis, N. J., and Messing, I.: Near-saturated hydraulic conductivity in soils of contrasting texture measured by tension
542 infiltrometers, *Soil Science Society of America Journal*, 59, 27–34, 1995.
- 543 Jarvis, N. J.: A review of non-equilibrium water flow and solute transport in soil macropores: principles, controlling factors
544 and consequences for water quality, *European Journal of Soil Science*, 58, 523–546,
545 doi:10.1111/j.1365-2389.2007.00915.x, 2007.
- 546 Koener, R.: *Quantile Regression*, Cambridge University Press, New York, 2005.
- 547 Kosugi, K.: Lognormal distribution model for unsaturated soil hydraulic properties, *Water Resources Research*, 32, 2697–
548 2703, doi:10.1029/96wr01776, 1996.
- 549 Landcare Research, S-map - New Zealand's national soil layer: <http://smap.landcareresearch.co.nz>, 2015.
- 550 Leij, F. J., Alves, W. J., van Genuchten, M. T., and Williams, J. R.: The UNSODA unsaturated soil hydraulic database, in:
551 *Proceedings of the International Workshop on Characterization and Measurement of the Hydraulic Properties of
552 Unsaturated Porous Media*, 1269–1281, 1999.
- 553 Leij, F. J., Haverkamp, R., Fuentes, C., Zatarain, F., and Ross, P. J.: Soil water retention: II. Derivation and application of
554 shape index, *Soil Science Society of America Journal*, 69, 1891–1901, doi:10.2136/sssaj2004.0226, 2005.
- 555 Lilburne, L. R., Hewitt, A. E., and Webb, T. W.: Soil and informatics science combine to develop S-map: a new generation
556 soil information system for New Zealand, *Geoderma*, 170, 232–238, doi:10.1016/j.geoderma.2011.11.012, 2012.
- 557 Lilly, A., Nemes, A., Rawls, W. J., and Pachepsky, Y. A.: Probabilistic approach to the identification of input variables to
558 estimate hydraulic conductivity, *Soil Science Society of America Journal*, 72, 16–24, doi:10.2136/sssaj2006.0391,
559 2008.
- 560 [Mbonimpa, M., Aubertin, M., Chapuis, R. P. and Bussi re, B.: *Practical pedotransfer functions for estimating the saturated
561 hydraulic conductivity, *Geotechnical and Geological Engineering*, 20\(3\), 235–259, doi:10.1023/A:1016046214724,
562 2002.*](#)
- 563 McKenzie, N., and Jacquier, D.: Improving the field estimation of saturated hydraulic conductivity in soil survey, *Australian
564 Journal of Soil Research*, 35, 803–825, doi:10.1071/s96093, 1997.
- 565 McKenzie, N. J., and Cresswell, H. P.: Field sampling. In: *Soil Physical Measurement and Interpretation for Land
566 Evaluation*, CSIRO, Collingwood, Victoria, 2002
- 567 McLeod, M., Aislabie, J., Ryburn, J., and McGill, A.: Regionalizing potential for microbial bypass flow through New
568 Zealand soils, *Journal of Environmental Quality*, 37, 1959–1967, doi:10.2134/jeq2007.0572, 2008.

- 569 McNeill, S., Webb, T., and Lilburne, L.: Analysis of soil hydrological properties using S-map data., Landcare Research
570 report 977, 2012.
- 571 Messing, I., and Jarvis, N. J.: Temporal variation in the hydraulic conductivity of a tilled clay soil as measured by tension
572 infiltrometers, *Journal of Soil Science*, 44, 11–24, 1993.
- 573 Patil, N. G., and Rajput, G. S.: Evaluation of water retention functions and computer program "ROSETTA" in predicting soil
574 water characteristics of seasonally impounded shrink-swell soils, *Journal of Irrigation and Drainage
575 Engineering-ASCE*, 135, 286–294, doi:10.1061/(asce)ir.1943-4774.0000007, 2009.
- 576 Pollacco, J. A. P.: A generally applicable pedotransfer function that estimates field capacity and permanent wilting point
577 from soil texture and bulk density, *Canadian Journal of Soil Science*, 88, 761–774, 2008.
- 578 Pollacco, J. A. P. and Angulo-Jaramillo, R.: A Linking Test that investigates the feasibility of inverse modelling: Application
579 to a simple rainfall interception model for Mt. Gambier, southeast South Australia, *Hydrological Processes*, 23(14),
580 2023–2032
- 581 Pollacco, J. A. P., Braud, I., Angulo-Jaramillo, R. and Saugier, B.: A Linking Test that establishes if groundwater recharge
582 can be determined by optimising vegetation parameters against soil moisture, *Annals of Forest Science*, 65(7)
- 583 Pollacco, J. A. P., Ugalde, J. M. S., Angulo-Jaramillo, R., Braud, I. and Saugier, B.: A Linking Test to reduce the number of
584 hydraulic parameters necessary to simulate groundwater recharge in unsaturated soils, *Adv Water Resour*, 31(2), 355–
585 369, doi:10.1016/j.advwatres.2007.09.002, 2008b.
- 586 Pollacco, J. A. P., Nasta, P., Ugalde, J. M. S., Angulo-Jaramillo, R., Lassabatere, L., Mohanty, B. P., and Romano, N.:
587 Reduction of feasible parameter space of the inverted soil hydraulic parameters sets for Kosugi model, *Soil Science*,
588 SS-S-12-00268, 2013.
- 589 Romano, N. and Nasta, P.: How effective is bimodal soil hydraulic characterization? Functional evaluations for predictions
590 of soil water balance, *Eur. J. Soil Sci.*, 67(4), 523–535, doi:10.1111/ejss.12354, 2016.
- 591 Romano, N., Nasta, P., Severino, G. and Hopmans, J. W.: Using Bimodal Lognormal Functions to Describe Soil Hydraulic
592 Properties, *Soil Sci. Soc. Am. J.*, 75(2), 468–480, doi:10.2136/sssaj2010.0084, 2011.
- 593 Rogowski, A. S.: Watershed physics – model of soil moisture characteristic, *Water Resources Research*, 7, 1575–1582, 1971
594 doi:10.1029/WR007i006p01575, 1971.
- 595 Rubio, C. M.: Applicability of site-specific pedotransfer functions and ROSETTA model for the estimation of dynamic soil
596 hydraulic properties under different vegetation covers, *Journal of Soils and Sediments*, 8, 137–145,
597 doi:10.1065/jss2008.03.281, 2008.
- 598 Schaap, M. G., and van Genuchten, M. T.: A modified Mualem-van Genuchten formulation for improved description of the
599 hydraulic conductivity near saturation, *Vadose Zone Journal*, 5, 27–34, 2006.
- 600 ter Braak, C. J. F., and Vrugt, J. A.: Differential evolution Markov chain with snooker updater and fewer chains, *Statistics
601 and Computing*, 4, 435–446, 2008.
- 602 van Genuchten, M. T.: Closed-form equation for predicting the hydraulic conductivity of unsaturated soils, *Soil Science
603 Society of America Journal*, 44, 892–898, 1980.
- 604 van Genuchten, M. T., Leij, F. J., and Yates, S. R.: The RETC code for quantifying the hydraulic functions of unsaturated
605 soils, *The RETC Code for Quantifying the Hydraulic Functions of Unsaturated Soils*, U.S. Department of Agriculture,
606 Agricultural Research Service 1991.
- 607 Vervoort, R. W., and Cattle, S. R.: Linking hydraulic conductivity and tortuosity parameters to pore space geometry and
608 pore-size distribution, *Journal of Hydrology*, 272, 36–49, 2003.
- 609 Watt, J. P. C., and Griffiths, E.: Correlation of hydraulic conductivity measurements with other physical properties New
610 Zealand, *New-Zealand Soil Bureau Commentaries*, 1983, 198–201, 1988.
- 611 Webb, T. H., Claydon, J. J., and Harris, S. R.: Quantifying variability of soil physical properties within soil series to address
612 modern land-use issues on the Canterbury plains, New Zealand, *Australian Journal of Soil Research*, 38, 1115–1129,
613 doi:10.1071/sr99091, 2000.
- 614 [Webb, T. H., Claydon, J. J. and Harris, S. R.: Quantifying variability of soil physical properties within soil series to address
615 modern land-use issues on the Canterbury Plains, *New Zealand Soil Res.*, 38\(6\), 1115–1129, doi:10.1071/SR99091.,
616 2000.](#)
- 617 Webb, T. H.: Identification of functional horizons to predict physical properties for soils from alluvium in Canterbury, New
618 Zealand, *Australian Journal of Soil Research*, 41, 1005–1019, doi:10.1071/sr01077, 2003.
- 619 Wösten, J. H. M., Lilly, A., Nemes, A., and Le Bas, C.: Final report on the EU funded project using existing soil data to
620 derive hydraulic parameters for simulation models in environmental studies and in land use planning, DLO Winand
621 Staring Centre, Wageningen, The Netherlands, 1998.
- 622 Wösten, J. H. M., Lilly, A., Nemes, A., and Le Bas, C.: Development and use of a database of hydraulic properties of
623 European soils, *Geoderma*, 90, 169–185, 1999.

624 Young, C. D.: Overview of ROSETTA for estimation of soil hydraulic parameters using support vector machines, Korean
625 Journal of Soil Science & Fertilizer, 42, 18–23, 2009.
626
627

628 **Tables**

629 **Table 1. Feasible range of the Kosugi parameters and θ_s which is θ measured at 5 kPa.**

630

	θ_s (cm ³ cm ⁻³)	θ_r (cm ³ cm ⁻³)	$\log_{10} h_m$ (cm)	σ (-)
Min	θ_s	0.0	1.23	0.8
Max	0.60	0.20	5.42	4.0

631

632

633 **Table 2. Description of the tortuosity parameters.**

634

Tortuosity	Description
τ_1	Takes into account the increased path length due to crookedness of the path. When $\tau_1 = 0$ the flow path is perfectly straight down. When τ_1 increases, the flow path is no longer straight but meanders.
τ_2	Theoretically represents the shape of a microscopic capillary tube. The τ_2 parameter is used to estimate restrictions in flow rate due to variations in pore diameter and pore shape. When $\tau_2 = 0$ the shape of the capillary tube is perfectly cylindrical. When τ_2 increases the tube becomes less perfectly cylindrical, which causes lower connectivity.
τ_3	High porosity soils tend to have large <i>effective pores</i> , $\theta_s - \theta_t$, which tend to be more connected than soils with smaller effective pores, which have more dead-ends. When $\tau_3 = 0$ the connectivity is the same between high and low porosity soils. When τ_3 increases the connectivity of the soil increases (Vervoort and Cattle, 2003; Pollacco et al., 2013). Pollacco et al. (2013) found τ_3 to be the least sensitive parameter.

635

636

637 **Table 3. Theoretical constraints of the K_{s_bim} model.**

638

Constraint	Explanation
$\theta_s \geq \theta_{s_mac} \gg \theta_r$	Self-explanatory.
$0 < \sigma_{mac} \leq 1.5$	To avoid any unnecessary overlap of θ_{bim} with θ_{bim_mat} .
$1 > \tau_1 > \tau_{1_mac} \geq 0$	Flow in the macropore domain (larger pores) is expected to be straighter than in the matrix domain (smaller pores) due to reduced crookedness of the path.
$1 > \tau_2 > \tau_{2_mac} \geq 0$	It is expected that the shape of the ‘microscopic capillary tube’ of the macropore domain (larger pores) is more perfectly cylindrical than in the matrix domain (smaller pores).
$1 > \tau_3 > \tau_{3_mac} \geq 0$	The macropore domain has larger pores, and therefore it is assumed that the pores are better connected than the matrix pores.

639

640

641 Table 4. Soil series and classification.

642

Region	Soil series	No. of horizons		New Zealand classification <i>Subgroup</i>	Soil taxonomy <i>Great group</i>
		<i>Topsoils</i>	<i>Subsoils</i>		
Canterbury regional study	Eyre	6	8	Weathered Orthic Recent	Haplustepts
	Templeton	9	17	Typic Immature Pallic	Haplustepts
	Wakanui	9	17	Mottled Immature Pallic	Humustepts
	Temuka	9	16	Typic Orthic Gley	Endoaquepts
	Lismore	7	5	Pallic Firm Brown	Dystrustepts
	Hatfield	9	18	Typic Immature Pallic	Humustepts
	Pahau	9	18	Mottled Argillic Pallic	Haplustalf
	Waterton	9	15	Argillic Orthic Gley	Endoaqualfs
Canterbury	Waimakariri		2	Weathered Fluvial Recent	Haplustepts
	Lismore		1	Pallic Orthic Brown	Dystrustepts
	Templeton		6	Typic Immature Pallic	Haplustepts
	Wakanui		2	Mottled Immature Pallic	Humustepts
	Temuka		2	Typic Orthic Gley	Endoaquepts
Manawatu	Hautere		3	Acidic Orthic Brown	Dystrudepts
	Levin		4	Pedal Allophanic Brown	Humudepts
	Levin mottled		4	Mottled Allophanic Brown	Humudepts
	Manawatu		1	Weathered Orthic Recent	Haplustepts
	Paraha		3	Mottled Immature Pallic	Haplustepts
	Westmere		2	Typic Mafic Melanic	Humudepts
Marlborough	Brancott		3	Mottled Fragic Pallic	Haplustepts
	Broadridge		3	Mottled-argillic Fragic Pallic	Haplustalf
	Grovetown		3	Typic Orthic Gley	Endoaquepts
	Raupara		1	Typic Fluvial Recent	Ustifluent
	Wairau		1	Typic Fluvial Recent	Ustifluent
	Woodburn		2	Pedal Immature Pallic	Ustochrept
Otago	Dukes		1	Typic Orthic Gley	Endoaquepts
	Linnburn		2	Alkaline Immature Semiarid	Haplocambids
	Matau		4	Typic Orthic Gley	Endoaquepts
	Otokia		1	Mottled Fragic Pallic	Haplustepts
	Pinelheugh		2	Pallic Firm Brown	Eutrudepts
	Ranfurlly		2	Mottled Argillic Semiarid	Haploargids
	Tawhiti		2	Pallic Firm Brown	Eutrudepts
	Tima		2	Typic Laminar Pallic	Haplustepts
	Waenga		2	Typic Argillic Semiarid	Haploargids
	Wingatui		2	Weathered Fluvial Recent	Haplustepts
Southland	Waikiwi		2	Typic Firm Brown	Humudepts
	Waikoikoi		2	Perch-gley Fragic Pallic	Fragiaqualfs

643

644
645
646

Table 5. Different combinations of texture, layer and The RMSE_{log10} reported by using K_{s_bim} and K_{s_uni} models, by stratifying the data with/without texture and layers:

Data stratification with Model form	RMSE_{log10}		
	K_{s_uni}	K_{s_bim}	$K_{s_bim} - K_{s_uni}$
Model with combined texture & layer All data combined	0.583	0.560	0.023
Model with Loam & clay (texture) (loam & clay)	0.577	0.543	0.034
Model with Topsoil & subsoil (layers)	0.450	0.430	0.020

648
649
650
651
652

653 **Table 6. Optimal tortuosity parameters of K_{s_uni} and K_{s_bin} .**

654

		N	RMSE_{log10}	T₁	τ_2	τ_3	T_{1_mac}	τ_{2_mac}	τ_{3_mac}	σ_{mac}
K_{s_bin}	Topsoil	51	0.232	5.007	0.969	0.787	4.734	0.511	0.041	0.322
	Subsoil	181	0.471	6.444	0.859	0.408	3.973	0.642	0.729	1.272
K_{s_uni}	Topsoil	51	0.259	5.859	0.967	0.530	-	-	-	-
	Subsoil	181	0.491	6.484	0.854	0.316	-	-	-	-

655

656

657

658 **Table 7. Descriptive statistics of the optimized θ_{mac} ($\theta_s - \theta_{s,\text{mac}}$), θ_s , h_m and σ Kosugi hydraulic parameters. The bar represents the**
 659 **average value, SD the standard deviation and N the number of measurement points.**

660

	N	$\overline{\theta_{\text{mac}}}$	$SD \theta_{\text{mac}}$	$\overline{\theta_s}$	$SD \theta_s$	$\overline{\theta_{s,\text{mac}}}$	$SD \theta_{s,\text{mac}}$	$\overline{\ln h_m}$	$SD \ln h_m$	$\overline{\sigma}$	$SD \sigma$	$\overline{K_s}$	$SD K_s$
		$(\text{cm}^3 \text{ cm}^{-3})$		$(\text{cm}^3 \text{ cm}^{-3})$		$(\text{cm}^3 \text{ cm}^{-3})$		(cm)		$(-)$		(cm h^{-1})	
Topsoil	51	0.038	0.035	0.48	0.04	0.45	0.04	6.43	1.02	3.00	0.61	167.	101.
Subsoil	181	0.030	0.030	0.42	0.05	0.39	0.06	5.39	1.66	2.64	0.86	19.	42.

661

662 **Table 8. Summary of the quantile regression fit of the log-transformed residuals.**

663

Quantile	a_0		a_1	
	Estimate	95% CI	Estimate	95% CI
$\tau = 0.025$	-0.476	$[-\infty, -0.44]$	-0.574	$[-0.62, \infty]$
$\tau = 0.500$	0.041	$[-0.036, 0.080]$	0.041	$[-0.093, 0.053]$
$\tau = 0.975$	0.357	$[0.332, \infty]$	0.627	$[-\infty, 0.711]$

664

665

666

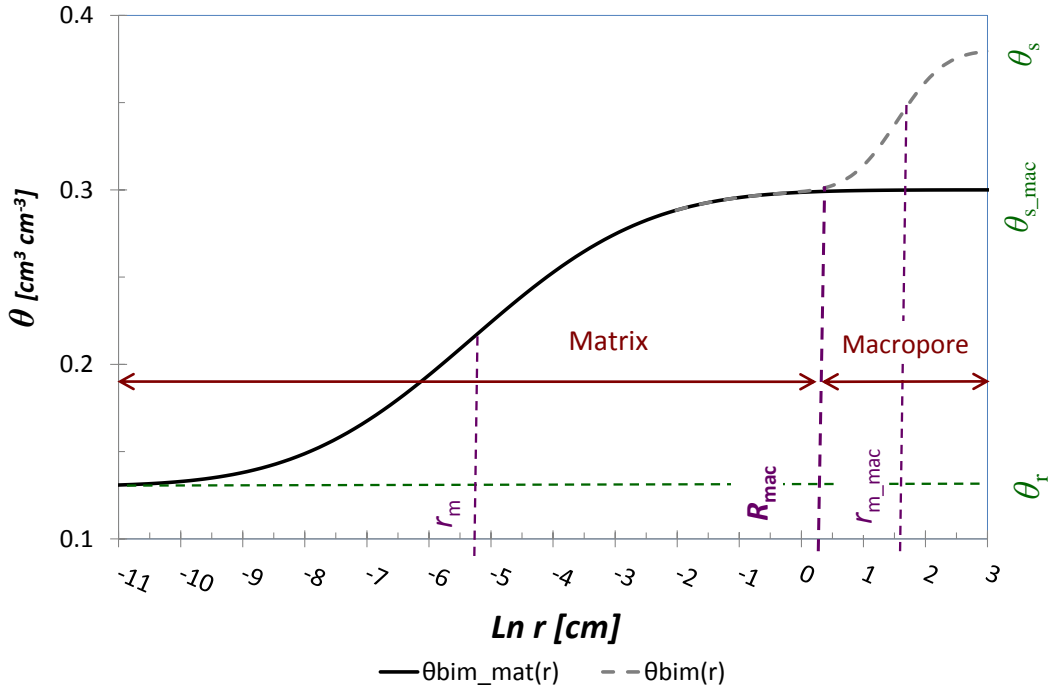
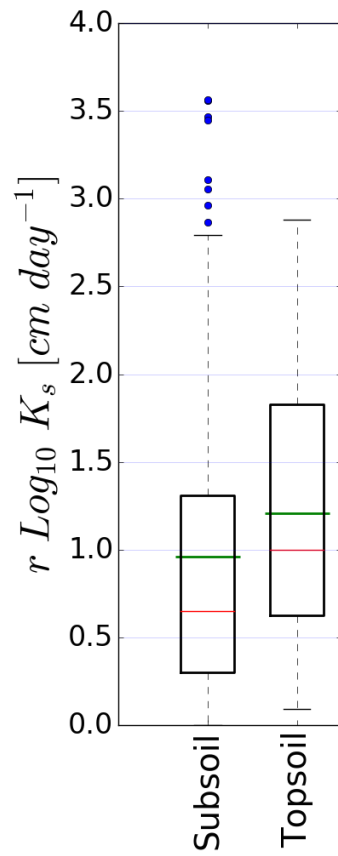


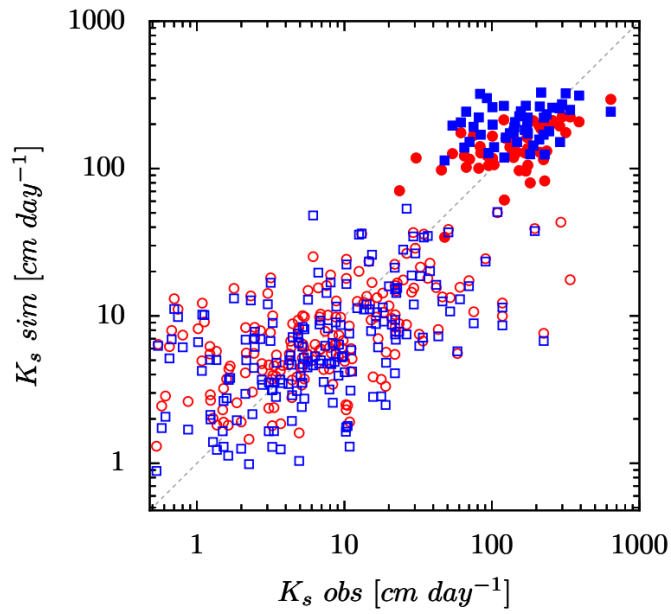
Figure 1. A typical Kosugi $\theta_{\text{bim}}(r)$ (Eq. (10a)) and $\theta_{\text{bim_mat}}(r)$ (Eq. (10b)) with the matrix and macropore domains and the positions of θ_s , θ_{s_mac} , θ_r , r_m , r_{m_mac} , R_{mac} shown.



672

673 Figure 2. Uncertainty of the standard error of the observed K_s in topsoil and subsoil. The lines in the box show upper and lower
 674 quartiles, the median (red), and mean (green). Whiskers show values within 1.5 times the quartile spread; values outside this range
 675 are shown as plotted points.

676



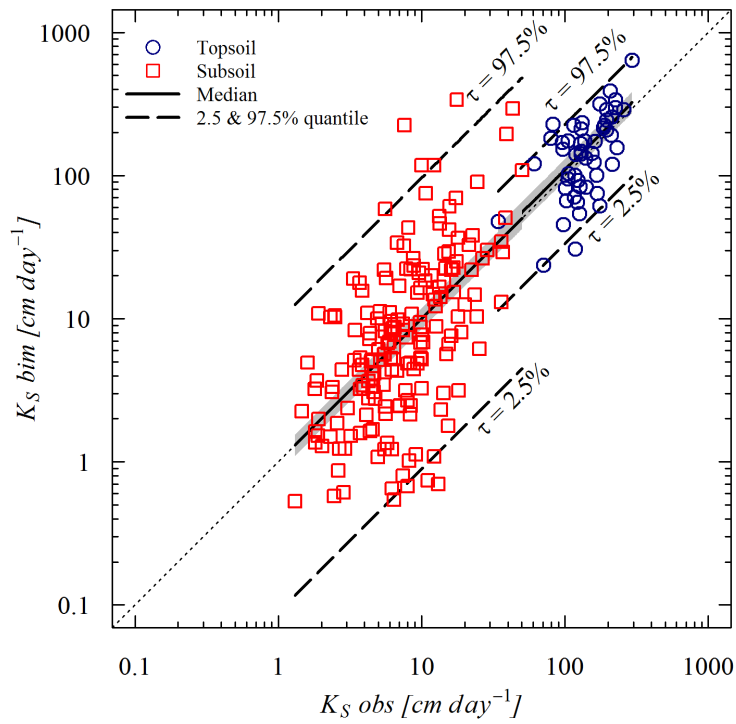
○ K_s bim/subsoil □ K_s uni/subsoil
● K_s bim/topsoil ■ K_s uni/topsoil

677

678

Figure 3. Plot between K_{s_obs} against K_{s_bim} and K_{s_uni} for topsoil and subsoil. The dotted line refers to the 1:1 line.

679



680

681

682

683

684

685

686

Figure 4. Error of $K_{s, bim}$ plotted against $K_{s, obs}$ for topsoil and subsoil. The solid line refers to the median line for each group, the dashed line refers to the upper or lower 95% confidence interval lines, the dotted line refers to the 1:1 correspondence line, and the shaded region is the 95% confidence interval of the median estimate.